Title

Beam on Nonlinear Winkler Foundation and Modified Neutral Plane Solution for Calculating Downdrag Settlement

Journal

Journal of Geotechnical and Geoenvironmental Engineering, 139(9)

ISSN

1090-0241

Authors

Wang, Rui
Brandenberg, Scott J

Publication Date

2013-09-01

DOI

10.1061/(asce)gt.1943-5606.0000888

Peer reviewed

http://dx.doi.org/10.1061/(ASCE)GT.1943-5606.0000888

Beam on nonlinear Winkler foundation and modified neutral plane solution for calculating downdrag settlement

Rui Wang[1] and Scott J. Brandenberg[2], M.ASCE.

Abstract

Since the work of Fellenius (1972), the neutral plane solution has been widely used to estimate downdrag settlements and drag loads mobilized in piles in consolidating soil profiles. Pile settlement is typically assumed equal to soil settlement at the neutral plane depth computed based on effective stress conditions at the end of consolidation. This paper demonstrates that, in general, pile settlement is not equal to soil settlement at the neutral plane depth; rather it is the relative velocity between the pile and soil that is zero at the neutral plane depth. A beam on nonlinear Winkler foundation (BNWF) solution, in which the shaft friction capacity is updated as consolidation progresses, is utilized to demonstrate that pile settlement is not equal to soil settlement at the neutral plane depth because the neutral plane depth evolves as consolidation progresses. The BNWF solution also shows that pile settlement depends on drainage conditions, with more settlement occurring when consolidation occurs first near the top of the consolidating soil layer, and less settlement occurring when consolidation initiates at the bottom. A modified neutral plane solution that is amenable to hand calculation is formulated to account for the evolution of neutral plane depth on pile settlement. Finally, the proposed BNWF and modified neutral plane solutions are compared with measurements of downdrag settlement from a centrifuge test program. The proposed methods produced more accurate estimates of pile settlement than the traditional neutral plane solution.

[1] PhD Candidate, State Key Laboratory of Hydroscience and Engineering, Department of Hydraulic Engineering, Tsinghua University, Beijing, China
[2] Associate Professor and Vice Chair, Department of Civil and Environmental Engineering, University of California, Los Angeles 90095-1593, email: sjbrandenberg@ucla.edu (corresponding author)

Introduction

Pile foundations embedded in soil profiles that settle due to surcharge loading, ground water level drop, liquefaction, etc, are subject to increased axial loads (i.e., drag load) and/or pile head settlements (i.e., downdrag). Consolidation-induced downdrag and drag load have been the topic of numerous field studies utilizing instrumented piles (e.g., Bjerrum et al. 1969; Endo et al. 1969; Fellenius 1972, 1984; Poulos and Davis 1980). Based on field observations Fellenius (1972) developed the neutral plane solution, NPS, where the neutral plane is the depth of maximum axial load marking the transition between downward shaft friction and upward shaft friction. The neutral plane depth is typically computed by summing axial loads from the top down and from the bottom up, and by force equilibrium the neutral plane lies at the intersection of these two lines as shown in Fig. 1. Typically the shaft friction capacity, f_s, is assumed to be mobilized along the full length of the pile because small relative displacements between soil and pile are required to mobilize f_s. Based on the observation that shaft friction is mobilized in an upward direction when the pile settles more than the soil, and in a downward direction when the soil settles more than the pile, Fellenius (1972) postulated that the soil settlement and the pile settlement are identical at the neutral plane, and this approach has been widely used to calculate downdrag settlement.

Although the neutral plane concept has contributed significantly to our understanding of piles in settling ground, several assumptions made in its typical application may deviate from actual loading conditions. First, as soil expels pore water during consolidation the effective stress increases, thereby resulting in time- and depth-varying f_s and time-varying neutral plane depth. Second, shaft friction exhibits elasto-plasticity such that relative displacements between a pile and soil may be small enough to mobilize only a portion of the ultimate shaft friction capacity, whereas full mobilization (i.e., rigid-plastic response) is typically assumed. Third, tip resistance is often assumed to be constant whereas in reality it depends on pile tip settlement.

To address these assumptions, a number of studies have approached the downdrag problem using continuum numerical solutions (e.g., Esmail 1996; Lee and Ng 2004; Jeong et al. 2004; Hanna and Sharif 2006; Sun and Yan 2010). However, the interface between the soil and pile requires careful selection of contact elements, and the complexity of the three dimensional continuum solutions renders them poorly suited to routine use. Due to the computational complexity of modelling a soil continuum, other researchers have adopted a beam on nonlinear Winker foundation (BNWF) approach to the neutral plane problem in which t-z elements model soil-pile interaction and a beam-column models the pile (e.g., Wong and Teh 1995; Kim and Mission 2009). However, the properties of the interaction elements are typically time-invariant and therefore the evolution of shaft friction capacity and neutral plane depth with time is not modelled. Wong and Teh (1995) acknowledge this problem, and suggest using effective stress conditions at the time when downdrag is to be computed (often the end of primary consolidation) to define properties of the t-z materials. However, Boulanger and Brandenberg (2004) demonstrated that accounting for the evolution of shaft friction capacity and the associated changes in neutral plane depth can result in significant differences in estimated downdrag settlement.

Beam on Nonlinear Winkler Foundation Solution of Downdrag Problem

A schematic of a BNWF approach that removes many of the assumptions in the traditional NPS is shown in Fig. 2. The solution utilizes the TzLiq1 material model implemented in OpenSees (McKenna and Fenves 2001) along the length of the pile to model shaft friction, and beam column elements for the structural properties of the pile. End bearing in the BNWF analysis can be modeled in two different ways: (i) a Q-z element (e.g., QzSimple1 in OpenSees) can be used at the pile tip to capture variation in end bearing load with pile tip settlement, or (ii) an upward force may be applied at the pile tip to represent a constant end bearing resistance. A load may also be applied to the pile head. The TzLiq1 and QzSimple1 materials adopt a nonlinear plasticity formulation such that the backbone load transfer behavior closely matches published relations [Reese and O'Neill (1988) or Mosher (1984) for t-z behavior; Reese and O'Neill (1988) or Vijayvergiya (1977) for Q-z behavior. A complete description of the material model equations is beyond the scope of this paper, but can be found in Boulanger et al. (2003), and in the OpenSees documentation. The TzLiq1 material was implemented in OpenSees with the specific intention of modeling piles in liquefiable soils (hence its name), but it is equally well suited for modeling downdrag problems resulting from more traditional consolidation mechanisms.

The key feature that makes the TzLiq1 materials amenable to consolidation analysis is the relation between f_s (also called t_{ult} or t_u in the literature) and vertical effective stress in the soil, σ_v'. The TzLiq1 material assumes that f_s varies linearly with σ_v', and is zero when σ_v' is zero. This is an important improvement upon previous analysis approaches that utilized constant f_s, regardless of consolidation condition. The analysis proceeds by computing values of f_s at each node along the pile based on the initial effective stress condition and soil-pile interface friction angle. Subsequently, time- and depth-dependent values of σ_v' and soil settlement, S_z, are input to the free-ends of the t-z elements, and the f_s values are updated to be compatible with σ_v' at each increment.

A simple example problem consisting of a 20m long reinforced concrete pile embedded in a layer of clay (Fig. 3) is selected to demonstrate the BNWF downdrag solution, and for comparison with the traditional NPS. The uniform clay layer has a saturated unit weight of $20kN/m^3$, initial void ratio of 0.8, and coefficient of compressibility (m_v) of $2.22\times10^{-4}kPa^{-1}$. A 150kPa surcharge was applied at the surface of the clay layer, resulting in a uniform vertical strain of 3.3%, and an ultimate surface settlement of 0.67m.

The square pile with 0.4m side length (B) was modeled using elastic beam column elements with Young's modulus of 40GPa (consistent with typical reinforced concrete). The pile was discretized into 100 elements (101 nodes) evenly distributed along its length. The soil-pile interface friction angle δ was set as 28° and the at-rest earth pressure coefficient K_0 was set as 0.5. The ultimate soil-pile interface friction was calculated as $f_s = \sigma_v' K_0 \tan\delta$. The load transfer behavior followed Reese and O'Neill's (1988) relation for clay, and the value of z_{50} (i.e., the displacement at which half of the ultimate shaft friction is mobilized) was set to 0.0002m. The resulting load transfer curve is fairly stiff, and is consistent with empirical observations that ultimate shaft friction is mobilized at small relative displacements on the order of millimeters. At the tip of the pile, a constant upward load of 144 kN was imposed to simulate full development of the undrained tip resistance during downdrag. A constant upward load was selected instead of a Q-z element at the pile tip to facilitate a direct comparison with the traditional neutral plane solution. The geotechnical capacity of the pile can be calculated through the sum of fully mobilized upward shaft friction and tip resistance, which comes up to 995kN. The solution was computed for various values of pile head load within the geotechnical capacity prior to consolidation, ranging from 144 kN to 900 kN. The example pile has a rather low end bearing resistance. For design, piles are often founded in more competent strata to provide higher end bearing resistance. In such cases, the neutral plane may be near the pile tip, which would reduce or eliminate downdrag settlement.

The example problem was solved using three different types of drainage conditions: drainage through both the top and bottom of the clay layer (double drainage, DD), single drainage through the top (SDtop), and single drainage through the bottom (SDbottom).The consolidation solution followed the Fourier series expansion of Terzaghi's one dimensional consolidation theory:

$$u(z,t) = \frac{4p}{\pi} \sum_{n=0}^{\infty} \frac{1}{2n+1} \sin \frac{(2n+1)\pi z}{2H} \exp\left(-(2n+1)^2 (\frac{\pi^2}{4}) T_v \right) \quad (1)$$

where $u(z,t)$ is the excess pore pressure at depth z and time t, H is drainage path length, and T_v is the time factor defined as $T_v = \frac{C_v}{H^2} t$. Isochrones of the consolidation ratio, U_z, computed from Eq. 1 are shown in Fig. 4, and are also available in many soil mechanics text books (e.g., Holtz, Kovacs, and Sheahan 2011). Time- and depth-dependent values of vertical effective stress, $\sigma_v'(z,t)$ for the free end of the t-z elements were computed as $\sigma_v'(z,t) = \sigma_{vf}'(z) - u(z,t)$, where $\sigma_{vf}'(z)$ is the final vertical effective stress after consolidation at depth z. Utilizing Terzaghi's 1-D consolidation theory inherently neglects excess pore pressures caused by pile installation, and changes to soil permeability and compressibility during consolidation.

The soil settlement $S_{soil}(z,t)$ in the clay layer was acquired by integrating the vertical strain in the soil profile as the clay consolidates. Isochrones of the dimensionless settlement ratio computed by integrating U_z with depth are also shown in Fig. 4 based on the assumptions that double drainage boundary conditions apply, and settlement is zero at the bottom of the consolidating layer. Soil settlement profiles at a desired time can be computed by multiplying the appropriate settlement ratio by the ultimate surface settlement. Settlement ratio isochrones for single drainage conditions are not presented herein for brevity, but can easily be obtained using the methods described earlier.

The computed time- and depth-dependent values of $\sigma_v'(z,t)$ and $S_{soil}(z,t)$ were imposed on the free ends of the TzLiq1 elements, and solutions of pile settlement were computed using OpenSees. The UpdateMaterialStage command was utilized prior to the first load increment to initialize the TzLiq1 materials so that the initial capacities were tied to the initial effective stress values. Subsequently, the capacities were updated as the effective stresses increased during consolidation. Penalty constraints were used to enforce the imposed displacement boundary conditions, and convergence was based on the norm of the displacement residuals (i.e., NormDispIncr in OpenSees) with the tolerance set to 10^{-8}. A Newton-Raphson algorithm was used to iterate on an equilibrium displacement field for each loading increment. Solutions were computed using 800 increments to reach an average degree of consolidation beginning at 0% and ending at 99.9%, and an automatic substepping algorithm was utilized to reduce the step size when convergence did not occur in 25 Newton-Raphson iterations.

BNWF Computation Results

Figs. 5 to 7 show the soil settlement, effective stress, soil-pile friction, and axial pile load distributions at four different average degrees of consolidation (25%, 50%, 75% and 99.9%) for a pile head load of Q_d=445kN. The depth of the neutral plane is clearly evident at the abrupt transition from negative to positive friction, and also at the depth of the maximum axial load. The profiles in Figs. 5-7 are identical at the end of primary consolidation, but differences in the profiles arise at intermediate degrees of consolidation.

In the double drainage case, effective stress initially builds up at both the top and bottom of the clay layer, causing soil strain and increase in soil-pile friction to be more prominent at the top and bottom. The increase in friction at the top serves to partially offset the increase in friction at the bottom, and the depth of the neutral plane remains nearly constant at slightly deeper than

10m as consolidation evolves. On the other hand, for the case with single drainage through the top the friction increases more quickly at the top of the pile, which shifts the neutral plane upward. As consolidation progresses, friction increases with depth along the pile and the neutral plane shifts downward to its final equilibrium depth at the end of consolidation. Conversely, when single drainage occurs through the bottom the friction increases first at the bottom of the pile, which shifts the neutral plane downward, and it progresses upward to its final equilibrium position at the end of consolidation.

The depth to the neutral plane, and pile settlement at the neutral plane depth are plotted versus average degree of consolidation in Fig. 8. The pile was essentially rigid (elastic compression was only a fraction of a millimeter at the end of consolidation), so Fig. 8 can be interpreted as pile head settlement. For the double-drained case, the pile settlement increases approximately linearly with average degree of consolidation, reaching a final value of 0.306m. For the SDtop case, the initial incremental soil strains occur first near the surface such that soil settlement is nearly zero below the neutral plane depth, which causes a very slow initial pile settlement rate. However, with time, the neutral plane shifts upward as the downdrag stresses increase near the pile head, soil strains shift downward as consolidation progresses, and the pile settlement rate increases quickly. The pile settlement at the end of consolidation is 0.350m, which is 14% larger than the double-drained case. For the SDbottom case, the pile initially settles quickly because incremental soil strains are largest deep in the profile, below the neutral plane depth. However with time the incremental soil strains move upward, resulting in a reduction in pile settlement rate. The final pile settlement reaches 0.262m, which is 14% less than the double-drained case. The traditional NPS claims that the pile settlement is equal to the soil settlement at the depth of the neutral plane at the end of consolidation, which is 0.310m for the example problem. This value is close to the double-drained case, but differs from the SDtop and SDbottom cases by ±14%, which is a non-negligible amount.

Having investigated the effect of drainage conditions on the settlement of piles in consolidating soil, we now turn our attention to the influence of pile head loading. Using the same procedures mentioned above, the settlement of single piles subjected to varying head loads within their geotechnical capacity were calculated through both the BNWF method and traditional NPS under the three drainage conditions (Fig. 9). For all four solutions, the pile settlement increased as the pile head load increased because the head load shifted the neutral plane upward in the soil profile. The traditional NPS solution does not match any of the BNWF cases, though it corresponds more closely with the double drainage case than with the single-drainage cases.

Fundamental Error in Traditional Neutral Plane Solution

The BNWF solution of the example problem illustrates a fundamental error in the manner in which the NPS is typically utilized to estimate downdrag settlement. The fundamental error is that the neutral plane solution assumes that the pile settlement and soil settlement are equal at the depth of the neutral plane. However, it is the relative velocity, not the relative displacement that must be zero at the neutral plane depth. Consider the elastic perfectly-plastic material response shown in Fig. 10. The neutral plane is defined as the position along the pile where shaft friction transitions from upward to downward, and is therefore zero. The load transfer curve in Fig. 10 illustrates two different points on where shaft friction is equal to zero, but they are associated with different amounts of displacement. This clearly establishes that relative displacement between pile and soil is not necessarily equal to zero at the depth where shaft friction is zero.

The kinematic condition describing relative movement between soil and pile at the neutral plane depth can be easily defined by traditional one-dimensional rate independent plasticity theory. The yield function is defined as $f = |Friction| - f_s$, and the Kuhn-Tucker complementary conditions require that $\dot{z_p} sign(Friction) \cdot f = 0$, where $\dot{z_p}$ is the plastic displacement rate (e.g., Simo and Hughes 1998). In the elastic region where $f<0$, the Kuhn-Tucker conditions dictate that $\dot{z_p} = 0$, whereas in the plastic region where f=0, the Kuhn-Tucker conditions dictate that $\dot{z_p} \neq 0$. Extending these plasticity concepts to the neutral plane solution, the neutral plane is defined as the depth where shaft friction is zero, which corresponds to the elastic region where $f < 0$. Therefore $\dot{z_p}= 0$ at the neutral plane based on the Kuhn-Tucker complementary conditions. One-dimensional rate independent plasticity theory dictates that it is the relative plastic displacement **rate** between the soil and pile, $\dot{z_p}$, and not the relative displacement, $\underline{z_p}$, that must be zero at the neutral plane depth. Note that the condition when $\dot{z_p}= 0$ and $f=0$ also satisfies the Kuhn-Tucker complementary conditions. Therefore, $\dot{z_p} = 0$ does not necessarily indicate a condition of zero friction (e.g., consider the end of consolidation condition where soil and pile are not settling, but shaft friction is nevertheless mobilized along the pile). However, when friction is equal to zero, $\dot{z_p}$ must be zero as well.

Considering that the relative velocity must be zero at the neutral plane depth, pile settlement can be computed as the integral of soil settlement velocity, V_{soil}, at the neutral plane depth over time:

$$S_{pile}(z_{np}(t)) = \int_0^t V_{soil}(z_{np}(t),t)dt \tag{2}$$

where $z_{np}(t)$ is the depth of the neutral plane at time t, and $V_{soil}(z,t) = \dfrac{\partial S_{soil}(z,t)}{\partial t}$, $S_{soil}(z\ ,t)$ is the soil settlement at depth z and time t. For the special case where $z_{np}(t)$ is constant, the soil settlement would be equal to the pile settlement at the neutral plane depth. However, if $z_{np}(t)$ is not constant, the pile settlement will, in general, be different than the soil settlement at the neutral plane depth, and will depend on the evolution of the neutral plane depth over time. For typical consolidation problems, the neutral plane depth will change with time because the effective stresses at the soil-pile interface will change as consolidation evolves. The traditional NPS utilizes the end-of-consolidation neutral plane depth and does not account for the evolution of neutral plane depth over time, and computes an erroneous settlement as a result. On the other hand, the BNWF solution inherently includes shifting of the neutral plane depth due to discretization of time, the link between t-z properties and consolidation stress, and enforcement of force equilibrium in each increment.

Modified Neutral Plane Solution

Although the BNWF method correctly captures the evolution of neutral plane depth over time, and its influence on pile settlement, performing such a BNWF analysis is currently beyond the capabilities of software commonly used in geotechnical design. Therefore we now turn our attention to formulating a simple modification to the neutral plane solution that is amenable to spreadsheet calculation. The steps of the modified neutral plane solution are summarized in the flow chart in Fig. 11. The first step involves discretizing time into convenient intervals for solving the consolidation problem. Times should be selected to correspond to reasonably consistent average degrees of consolidation (e.g., times corresponding to U_{ave} = 0%, 25%, 50%, 75%, and 100% might be selected if five time steps are desired). Second, profiles of excess pore pressure and vertical strain are computed at each time using consolidation theory, and the settlement profile $S_{soil}(z_{np}(t_i),t_i)$ is computed by integrating the vertical strain profile from the bottom up (e.g., see Fig. 4). Third, the depth of the neutral plane is solved at each time interval in the traditional manner originally suggested by Fellenius (1972) in which forces are summed from the top down and bottom up, and the neutral plane depth lies at the intersection of the two lines. However, the shaft friction values must be based on the current effective stress at a particular depth based on the consolidation solution from step 2. The variation in shaft friction during consolidation is precisely why the neutral plane shifts with time, and is why the traditional NPS incorrectly predicts pile settlement. Fourth, the pile settlement at the neutral plane depth is computed by integrating soil settlement velocity at the neutral plane depth over time. Numerical discretization of time transforms the integral of velocity into a difference in incremental displacements. Hence, the pile settlement for a particular time step, n, can be computed using the forward Euler integration method in Eq. 3:

$$S_{pile}(z_{np}) = \sum_{i=1}^{n} \left[S_{soil}(z_{np}(t_{i+1}), t_{i+1}) - S_{soil}(z_{np}(t_{i+1}), t_i) \right] \quad (3)$$

For cases where elastic deformation of the pile is anticipated to be significant, axial strains must be integrated over the pile length to compute the contribution of pile shortening to head settlement. Furthermore, if a load-transfer curve (i.e., a Q-z relationship) is utilized rather than a constant specified tip resistance, iteration is required to obtain a tip resistance that is compatible with the current pile tip settlement.

The example problem presented in Figs. 5 through 7 was also analyzed using the modified NPS using various numbers of time steps (3, 5, and 33). The time steps were chosen to be at constant intervals of average degree of consolidation. Fig. 12 compares the BNWF method and the modified neutral plane method. The modified NPS accuracy increases as the number of time steps increases. The small differences between the modified NPS with 33 time steps and the

BNWF solution are likely attributed to differences in time discretization (800 time steps compared with 33) and elasto-plasticity of the t-z materials in the BNWF solution compared with the assumption of rigid plasticity in the modified NPS. Using a modest number of 5 time steps provides reasonable solutions for all three cases, and is reasonably approachable in a spreadsheet calculation.

Comparison with experimental data

To further validate the BNWF approach and modified NPS, a model pile from a centrifuge test by Lam et al. (2009) is analyzed. The centrifuge test was conducted at the Geotechnical Centrifuge Facilities at the Hong Kong University of Science and Technology to investigate axial load effects on piles in consolidating ground. The test program involved multiple pile foundations, but only one single pile test (test no. 1 in their paper) is analyzed here. The centrifugal acceleration was 60g and results are presented in prototype dimensions.

An instrumented tubular aluminium pile with an outer diameter (D) of 1.2m and wall thickness (t_{wall}) of 9cm was installed in an 18m thick layer of clay (Speswhite China clay) consolidated to a vertical effective stress of 80kPa before pile installation and spin up (Fig. 13). The clay rested atop a dense Leighton Buzzard sand layer that provided free drainage to the clay, another layer of sand atop the clay layer, resulting in a double-drained condition. The pile tip was 1.2m above the bottom of the clay layer. The top sand layer provided a surcharge of 45kPa, resulting in a measured 10 kN drag load on the pile from the sand. No load was applied to the pile head. The saturated unit weight, at-rest earth pressure coefficient, and initial void ratio of the clay were specified to be 16.3kN/m^3, 0.58, and 1.602 respectively. The coefficient of consolidation c_v was back calculated to be 5×10^{-7}m^2/s from the distributions of excess pore pressure measured in the test using Terzaghi’s one dimensional consolidation theory. Isochrones of predicted and measured excess pore pressure plotted in Fig. 13 show good agreement. The coefficient of compressibility $m_v = 3.63\times10^{-7}\mathrm{Pa}^{-1}$ was back calculated based on the measured soil surface settlement of 654mm.

In the BNWF simulations, the backbone of Reese and O'Neill's (1988) load transfer curve was used for the t-z elements. The soil-pile interface friction angle was estimated from the distribution of dragload after consolidation to be 24°. The value of z_{50} (displacement at which 50% of ultimate resistance is mobilized) was set to be 0.0005m, such that 99% of the shaft friction was mobilized at around 4~5mm.

A Q-z element was attached to the tip of the pile to model end bearing resistance. End bearing is a bit complicated for this problem because (i) it is unclear whether undrained or drained end bearing resistance would apply for the slow loading conditions induced during downdrag, and (ii) end bearing resistance would be anticipated to increase over time as the clay near the tip of the pile consolidates. Regarding (i), the test data can be used to provide some guidance since drained tip resistance is typically significantly larger than undrained tip resistance. Lam et al (2009) stated that prior to spin up, the soil was preloaded to 80kPa using a hydraulic press, resulting in an estimated undrained shear strength s_u of 17.6kPa prior to swelling of the clay, giving a strength ratio $\frac{s_u}{\sigma_v'} = 0.22$. Invoking concepts of normalization of undrained shear strength with consolidation stress and overconsolidation ratio (e.g., Ladd 1991), the undrained shear strength at the tip of the pile was estimated as $s_u = 0.22 \cdot \sigma_v' \cdot OCR^{0.8}$. The undrained shear strength prior to spin-up was estimated to be 9kPa, and the final undrained shear strength at the end of reconsolidation was estimated to be 35kPa based on the effective stress profiles in Fig. 14. Computing tip resistance as $Q_t = 10 S_u A$ the initial and final tip resistance came to 100kN and

400kN, respectively. At the end of consolidation, when the pile had settled significantly and clearly mobilized the ultimate tip resistance, the axial load at the tip of the pile was quite close to 400kN based on extrapolation from the deepest strain gauge measurement (Fig. 14). Although a bearing factor of 9 is commonly used for undrained tip resistance, many researchers suggest that it is too low and suggest a higher value ranging from about 9 to 12 (e.g., Salgado 2008), so the fact that a bearing factor of 10 agreed well with the data is not surprising. On the other hand, the drained bearing capacity would be significantly larger than the measurements [e.g., over 1300 kN is estimated using Meyerhof's (1976) bearing factors for a friction angle of only 20°]. Hence, we conclude that undrained tip resistance was mobilized during downdrag.

A Q-z element was attached to the pile tip, and the capacity of the element was increased from 100 kN to 400 kN in proportion to degree of consolidation at the pile tip elevation during consolidation. The z_{50} value was set to 0.012m such that the ultimate load is mobilized at approximately 8% of the pile diameter, which is consistent with the range presented by Reese and O'Neill (1988).

Fig. 14 shows the soil and pile responses at different average degrees of consolidation from the BNWF solution along with the final axial load distribution measured during the test. The final axial load distribution matches the centrifuge test data reasonably well. The final pile head settlement was estimated to be 0.194m (Fig. 15), which corresponds well with the measured settlement of 0.206m (-6% error).

In addition to the BNWF solution, the settlement was computed using the modified NPS with time discretization at U_{ave} = 0%, 25%, 50%, 75% and 100%. Iteration was used to match the properties of the same Q-z relation used in the BNWF solution. The final pile settlement using the modified NPS method was 0.208m, which is also very close to the measured settlement (+1%

error). On the other hand, the traditional NPS method predicts the pile settlement to be 0.277m (+34% error), which is significantly larger than the measured value and the values computed from the BNWF method and modified NPS method. The overprediction of the traditional NPS method is expected because the neutral plane begins near the tip of the pile and transitions upward as consolidation progresses. Using the final neutral plane position in the traditional NPS method therefore over-estimates pile settlement.

Conclusions

Pile settlement is typically assumed equal to soil settlement at the depth of the neutral plane, but this is a false inference; rather, the pile velocity is equal to the soil velocity at the neutral plane depth. This fact is supported by fundamental equations from one-dimensional rate independent plasticity theory. Pile displacement must be computed as the integral of soil settlement velocity at the neutral plane depth over time. If the neutral plane depth changes during consolidation (it typically does because interface friction depends on consolidation condition), the traditional neutral plane solution produces an inaccurate estimate of pile settlement. If the neutral plane depth is constant during consolidation, the traditional neutral plane solution is accurate.

An innovative new beam on nonlinear Winkler foundation approach was presented in which the shaft friction capacity evolves as effective stresses increase during consolidation. The new BNWF method clearly demonstrated the fundamental mechanisms involved in time-varying load transfer between pile and consolidating soil, and showed that settlements from the traditional neutral plane solution are generally inaccurate. A modified neutral plane solution that is amenable to spreadsheet calculation was formulated to account for evolution of the neutral plane depth over time, and provided reasonable agreement with the BNWF solutions.

When end-of-consolidation effective stress conditions are used to compute z_{np} in the traditional NPS, settlement will be under-predicted if z_{np} moves higher than the final z_{np} during consolidation, and over-predicted if z_{np} moves lower than the final z_{np}. The explanation is that settlement decreases with depth, so contributions to settlement at depths shallower than the final z_{np} tend to increase pile settlement compared with the traditional NPS. Although the evolution of the neutral plane depth affects downdrag settlement, it has no influence on the maximum dragload mobilized in the pile, which occurs at the end of primary consolidation.

Acknowledgments

The authors would like to thank the research group at Hong Kong University of Science and Technology for having performed high quality centrifuge tests and for publishing the data that was directly relevant to this paper. The authors would also like to thank National Natural Science Foundation of China (No. 51079074 and 51038007) and the Chinese Scholarship Council for providing the funding that enabled Rui Wang to visit UCLA to do the work presented herein. This material is based upon research performed in a renovated collaboratory by the National Science Foundation under Grant No. 0963183, which is an award funded under the American Recovery and Reinvestment Act of 2009 (ARRA).

References

Bjerrum L., Johannessen, I. J., Eide, O. (1969). "Reduction of negative skin friction on steel piles to rock". Proceedings 7th International Conference on Soil Mechanics and Foundation Engineering, Mexico City, August 25 - 29, Vol. 2, 27-34.

Boulanger, R.W., Brandenberg, S.J. (2004). "Neutral plane solution for liquefaction-induced downdrag on vertical piles". Proceedings ASCE Geo-Trans Conference, Los Angeles, California, 27-31.

Boulanger, R.W., Kutter, B.L., Brandenberg, S.J., Singh, P., and Chang, D. (2003). Pile Foundations in Liquefied and Laterally Spreading Ground during Earthquakes: Centrifuge Experiments and Analyses. Report No. UCD/CGM-03/01, Center for Geotechnical Modeling, Department of Civil Engineering, University of California, Davis, CA, 205 pp.

Endo M., Minou A., Kawasaki T., Shibata T. (1969). "Negative skin friction acting on steel piles in clay". Proc. 8th International Conference on Soil Mechanics and Foundation Engineering, Mexico City, August 25 - 29, Vol. 2, 85-92.

Esmail H. (1996). "Neutral plane of single piles in clay subjected to surcharge loading". M.S. thesis, Concordia University, Quebec, Canada.

Fellenius, B. H. (1972). "Downdrag on long piles in clay due to negative skin friction". Canadian Geotechnical Journal, 9(4), 323-337.

Fellenius, B. H., (1984). "Negative skin friction and settlement of piles". Proceedings of the Second International Seminar, Pile Foundations, Nanyang Technological Institute, Singapore, 1-12.

Hanna A. M., Sharif A. (2006). "Drag force on single piles in clay subjected to surcharge loading". International Journal of Geomechanics, 6(2), 89-96.

Jeong S., Lee J., Lee C. J. (2004). "Slip effect at the pile-soil interface on dragload". Computer and Geotechnics 31, 115-126.

Holtz R. D., Kovacs W. D., and Sheahan T. C. (2011). An Introduction to Geotechnical Engineering, 2nd Edition, Pearson Prentice-Hall, Upper Saddle River, New Jersey.

Kim H., Mission J. L. C. (2011). “Development of negative skin friction on single piles: uncoupled analysis based on nonlinear consolidation theory with finite strain and the load-transfer method”. Canadian Geotechnical Journal, 48(6), 905-914.

Ladd, C.C. (1991). "Stability Evaluation during Staged Construction." Journal of Geotechnical and Geoenvironmental Engineering. 117(4), 540-615.

Lam S. Y., Ng, C. W. W., Leung C. F., Chan, S. H. (2009). “Centrifuge and numerical modeling of axial load effects on piles in consolidating ground”. Canadian Geotechical Journal, 46: 10–24.

Lee C. J., Ng W. W. (2004). “Development of down-drag on piles and pile groups in consolidating soil”. Journal of Geotechnical and Geoenvironmental Engineering, 130 (9), 905-914.

McKenna F., and Fenves G. L. (2001). "OpenSees Manual." PEER Center, http://OpenSees.berkeley.edu.

Mosher R. L. (1984). "Load Transfer Criteria for Numerical Analysis of Axial Loaded Piles in Sand." US Army Engineering Waterways Experimental Station, Automatic Data Processing Center, Vicksburg, Mississippi, January.

Poulos H. G., and Davis E. H. (1980). Pile foundation analysis and design, Wiley, New York.

Reese, L. C. and O'Neill M. W. (1988). "Drilled Shafts: Construction Procedures and Design Methods." Report No. FHWA-HI-88-042, U.S. Department of Transportation, Federal Highway Administration, Office of Implementation, McLean, Virginia.

Salgado R. (2008). *The Engineering of Foundations*. 882p. McGraw Hill, New York.

Simo J. C. and Hughes T. J. R. (1998) Computational Inelasticity. Springer, Berlin Heidelberg New York.

Sun T. K., Yan W. M. (2010). “Development of neutral plane on a pile in a consolidating ground”. Proceedings of the 2nd International Symposium on Computational Mechanics, Hong Kong, Vol. 1233, 1594-1599.

Terzaghi K. (1925). Erdbaumechanik auf Bodenphysikalischer Grundlage, Franz Deuticke, Leipzig und Wein, 399p.; Structure and Volume of Voids of Soils, 10-13 (translated by A. Casagrande) in Terzaghi (1960).

Terzaghi K. (1960). From Theory to Practice in Soil Mechanics, Wiley, New York, 425.

Vijayvergiya V. N. (1977). "Load-Movement Characteristics of Piles." Proceedings, Ports 77 Conference, American Society of Civil Engineers, Long Beach, California, March.

Wong K. S. and Teh C. I. (1995). "Negative skin friction on piles in layered soil deposits". Journal of Geotechnical Engineering, 121 (6), 457-465.

Figure
Click here to download high resolution image

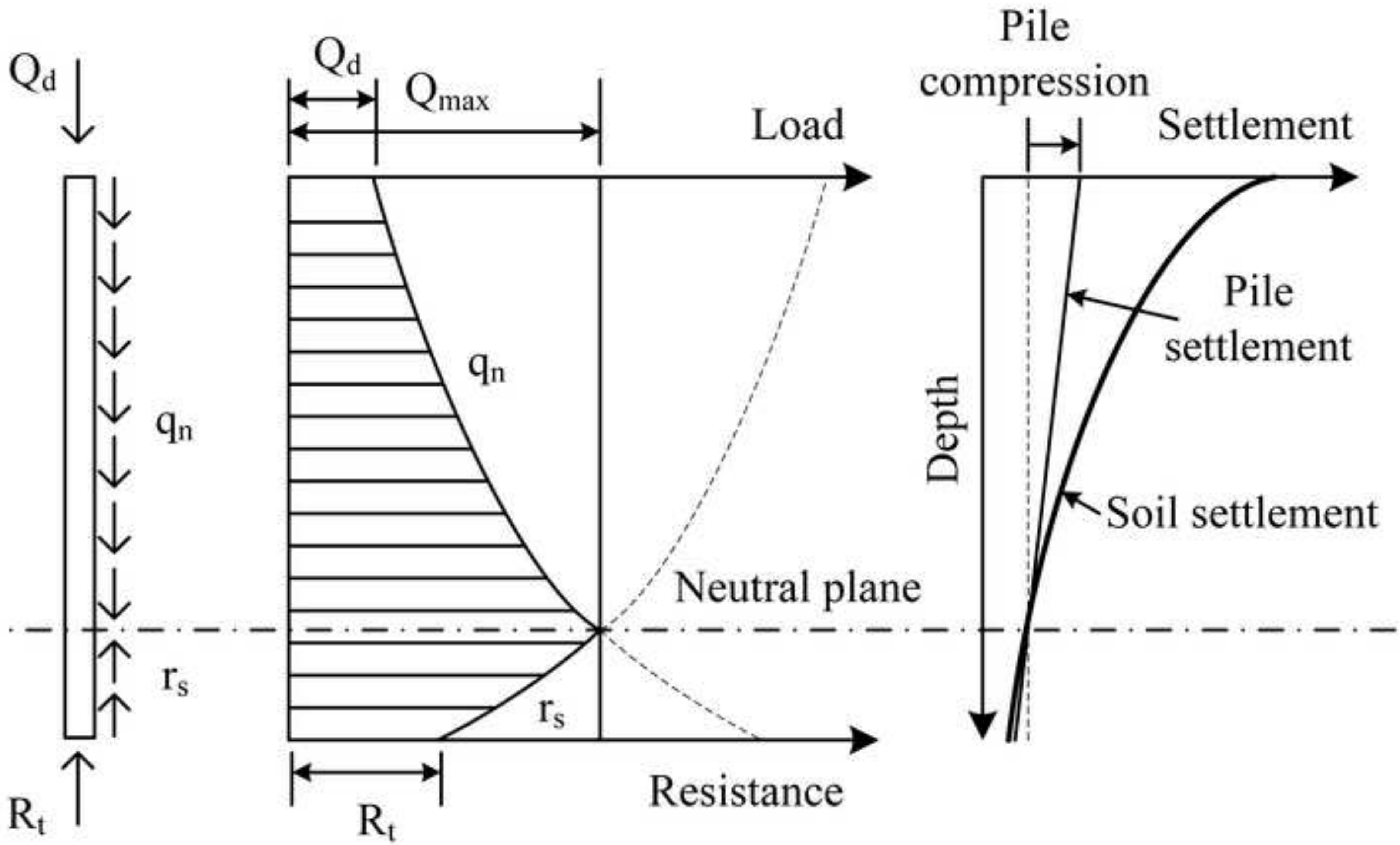

Figure 2
Click here to download high resolution image

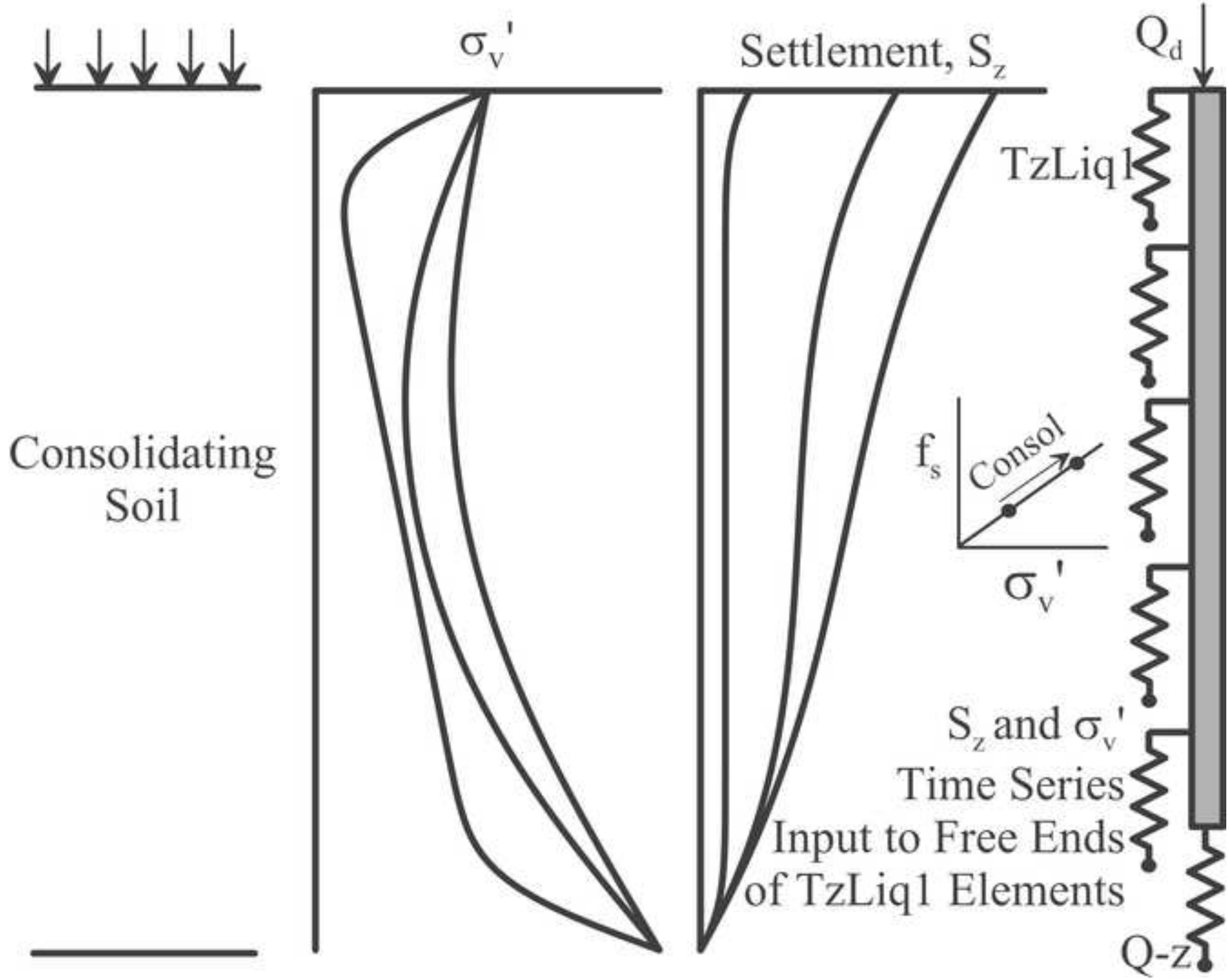

Figure 3
Click here to download high resolution image

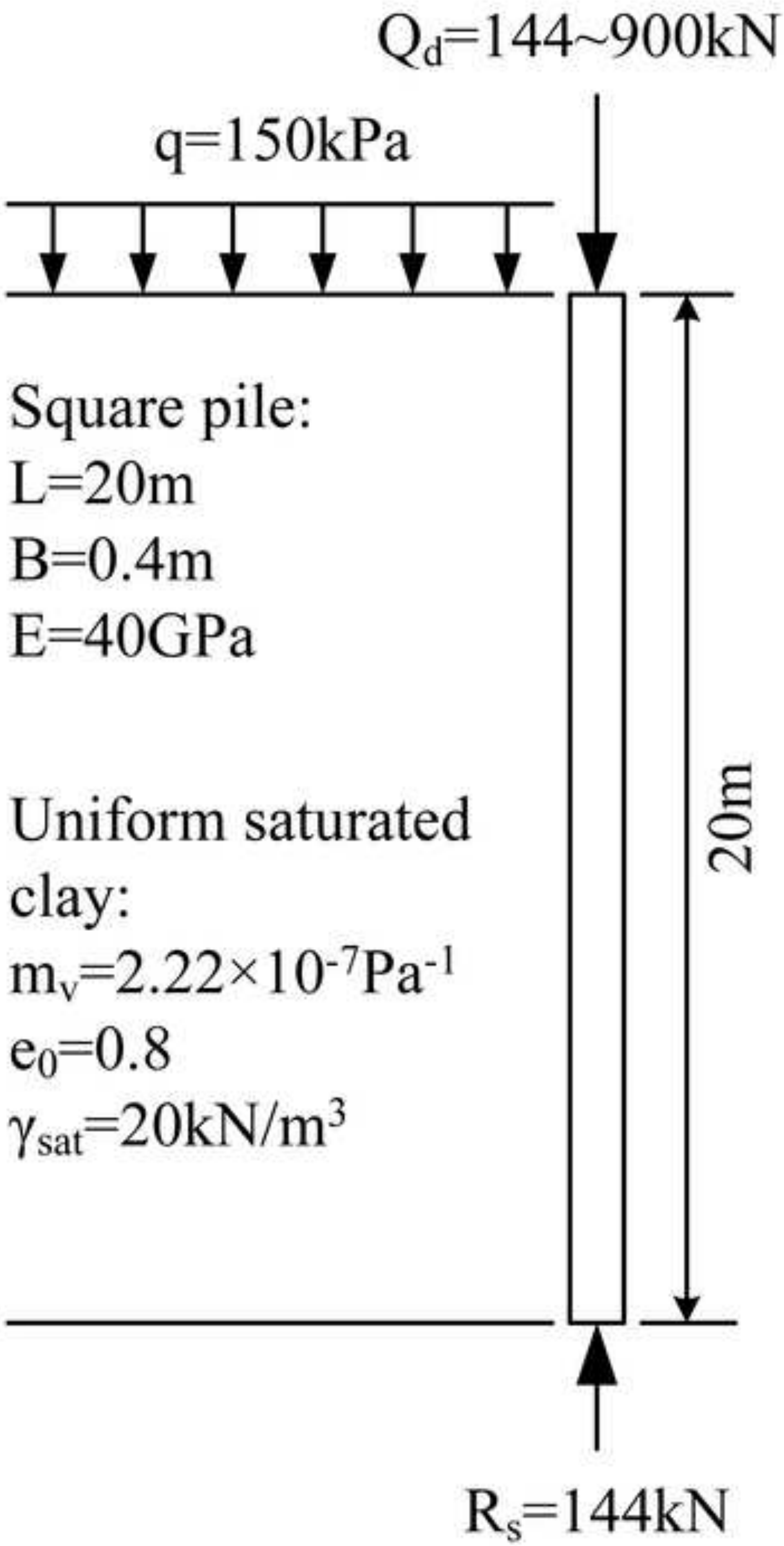

Figure 4
Click here to download high resolution image

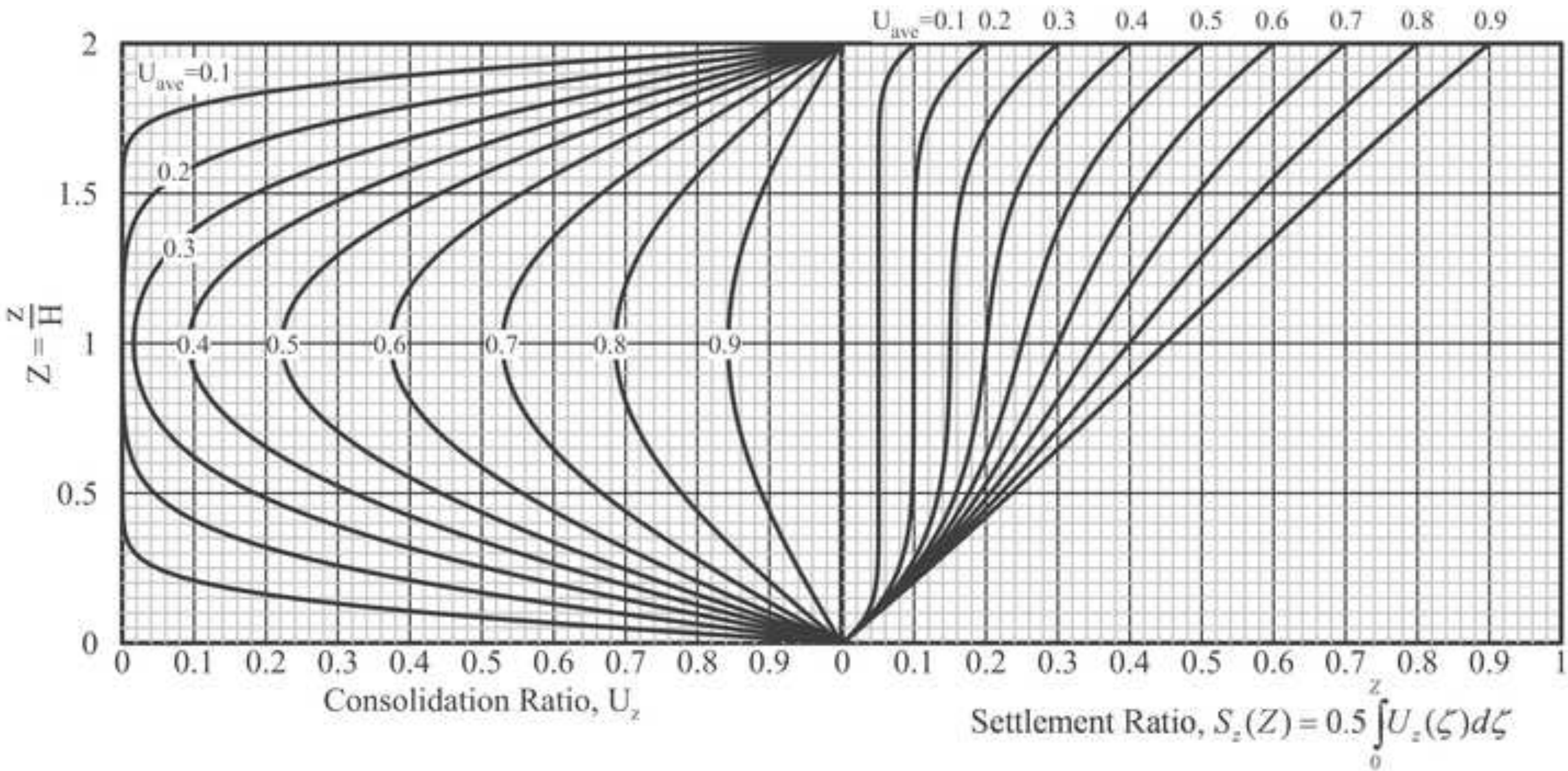

Figure 5
Click here to download high resolution image

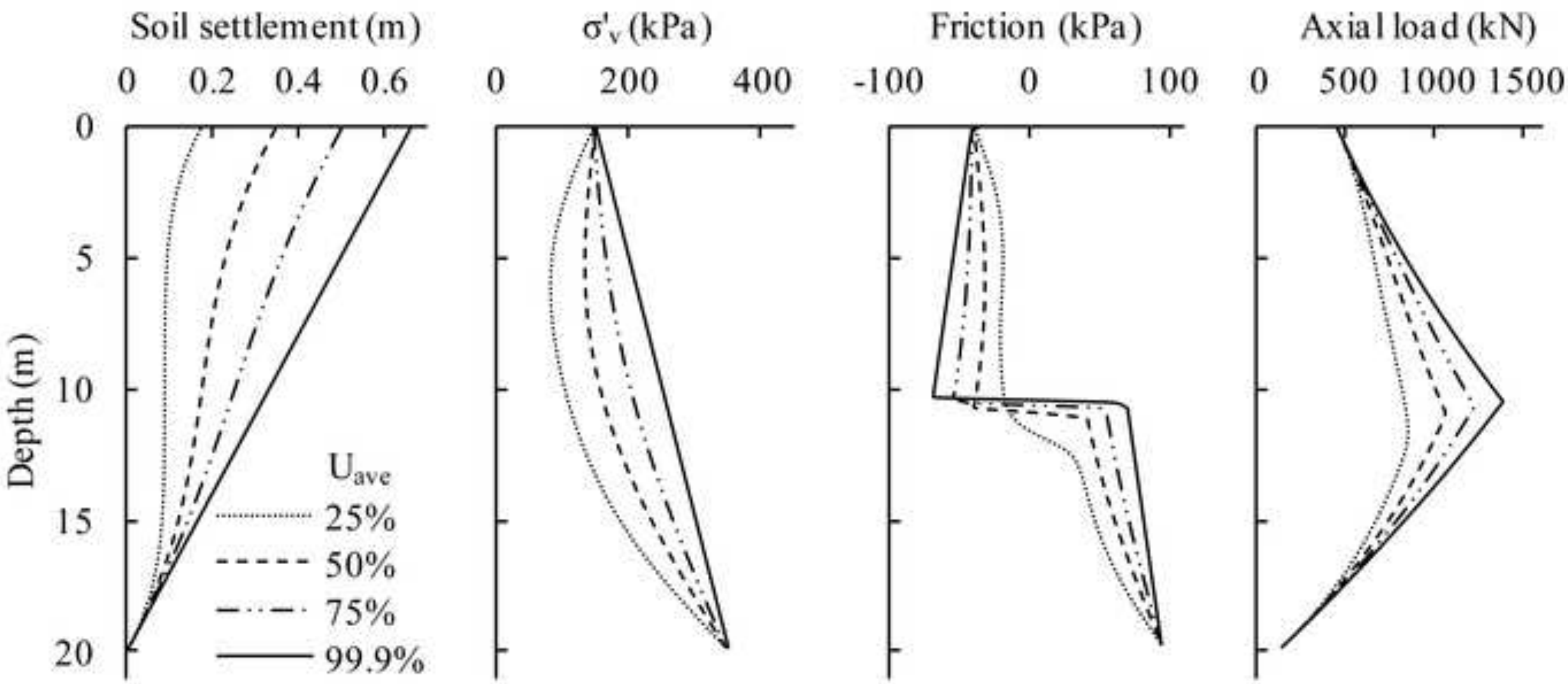

Figure 6

Click here to download high resolution image

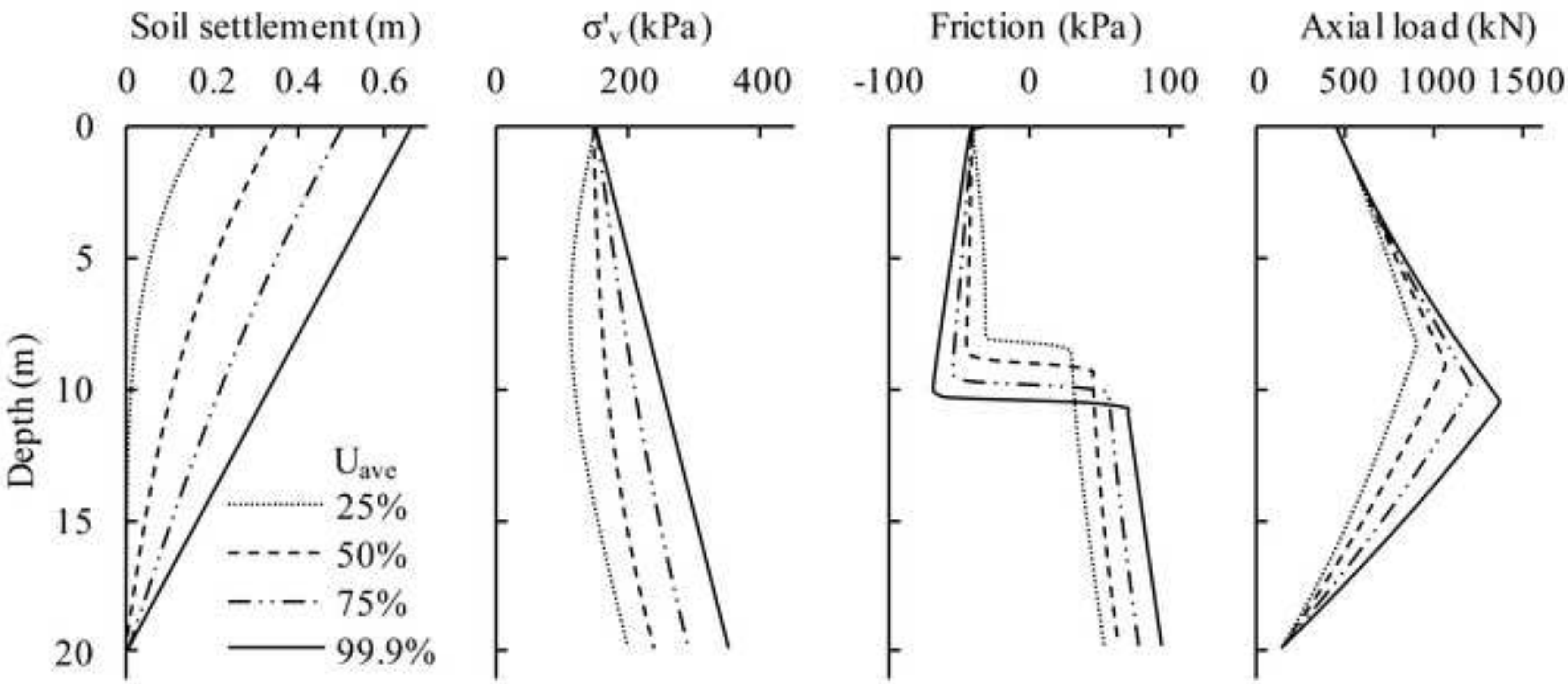

Figure 7
Click here to download high resolution image

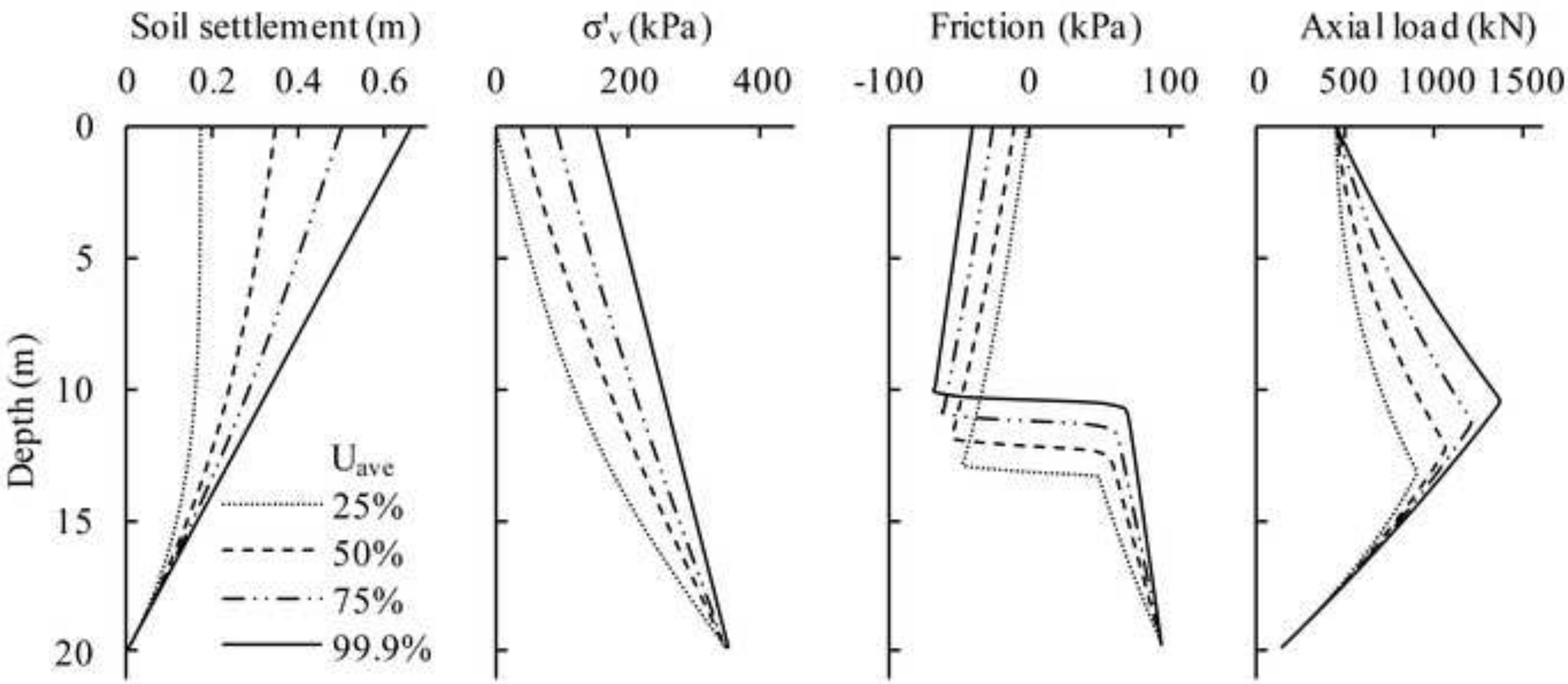

Figure 8
Click here to download high resolution image

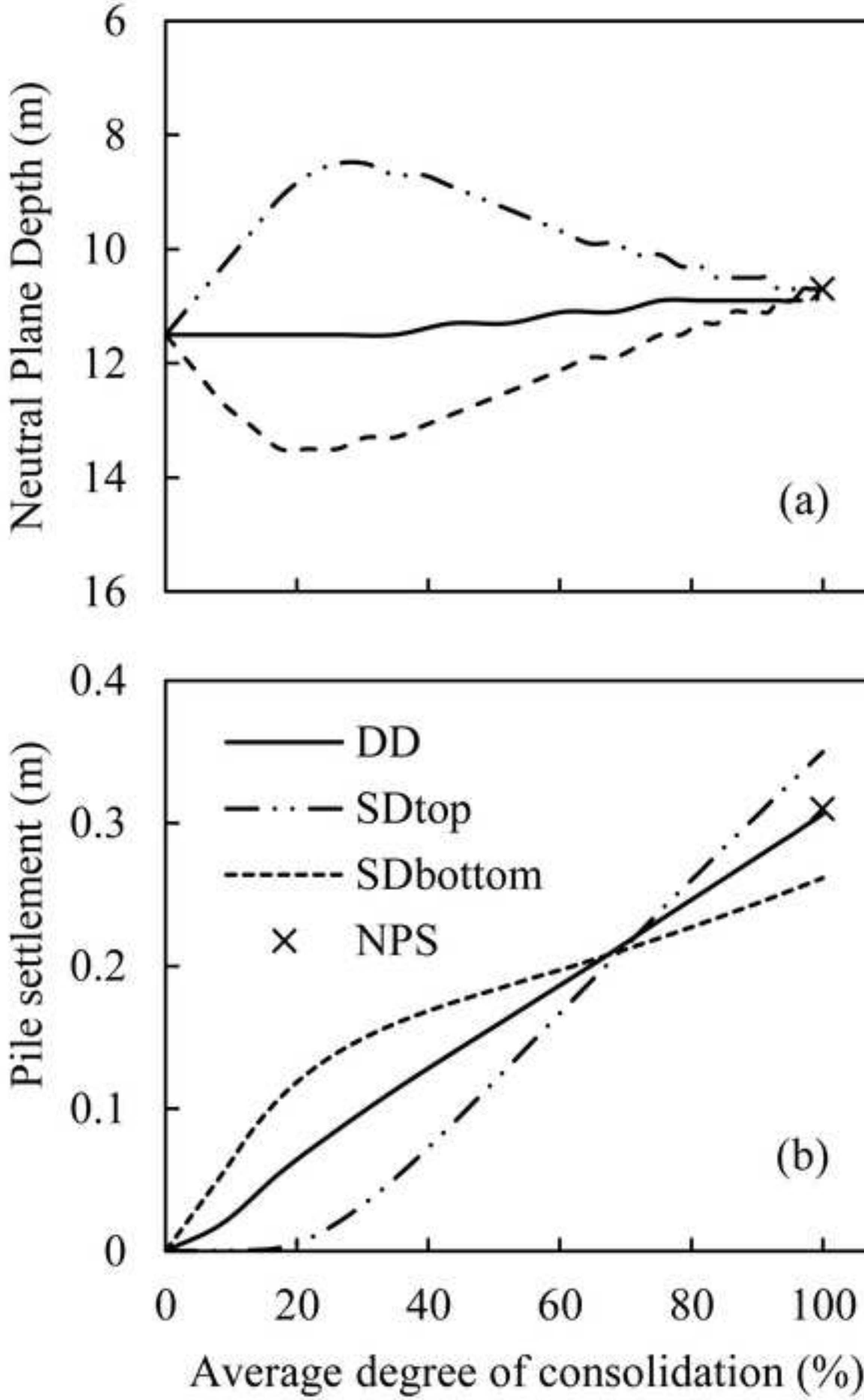

Figure 9
Click here to download high resolution image

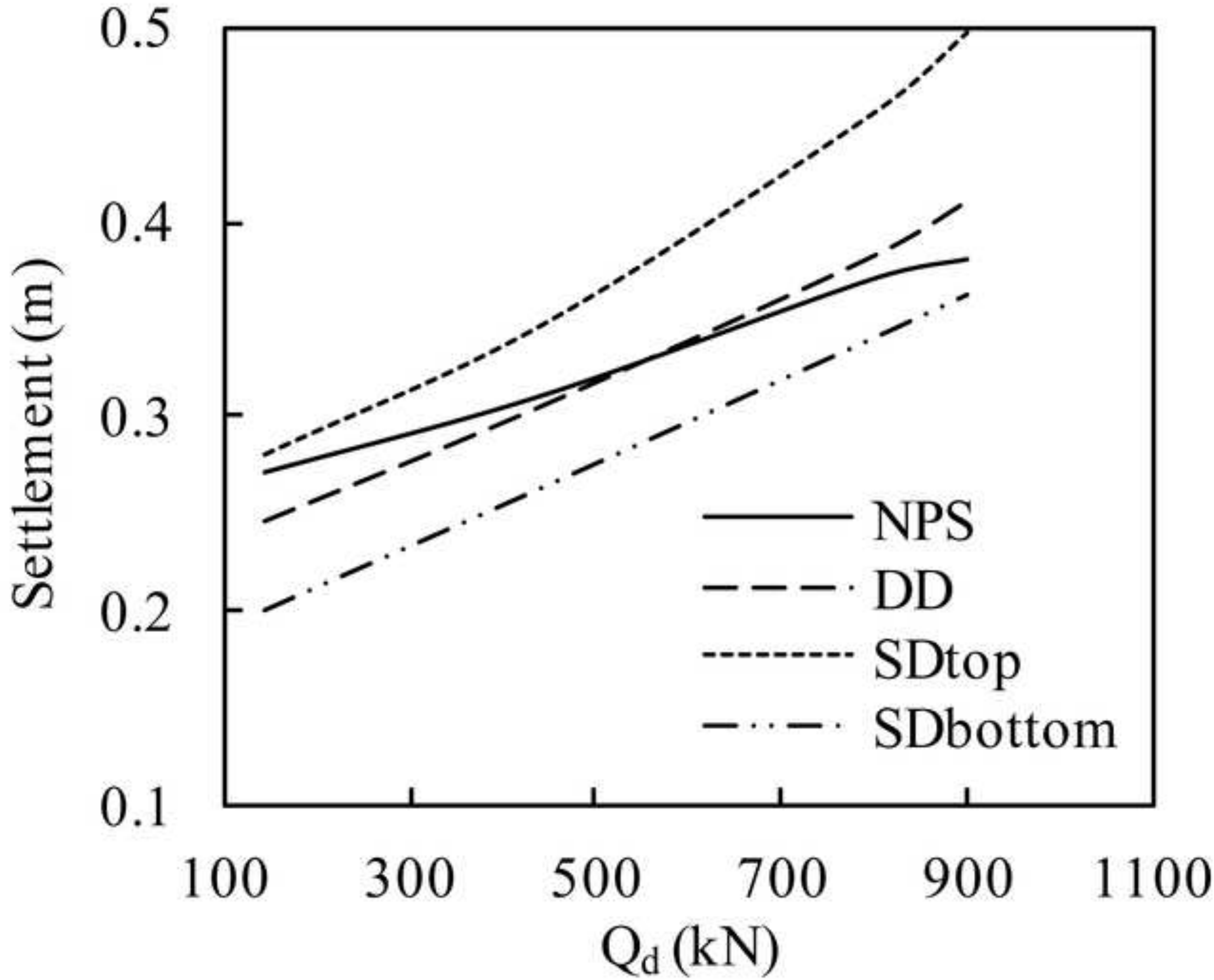

Figure 10
Click here to download high resolution image

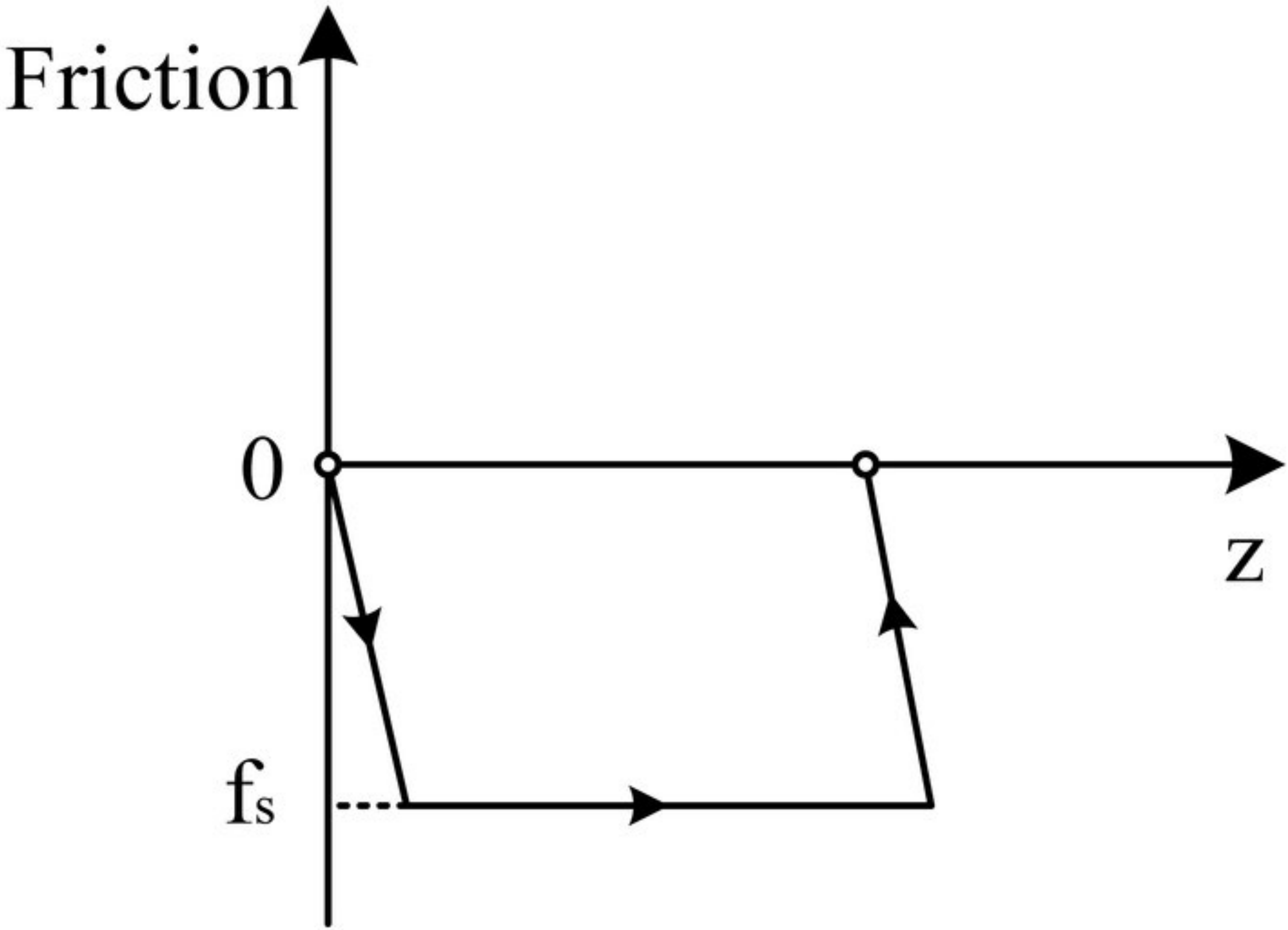

Figure 11
Click here to download high resolution image

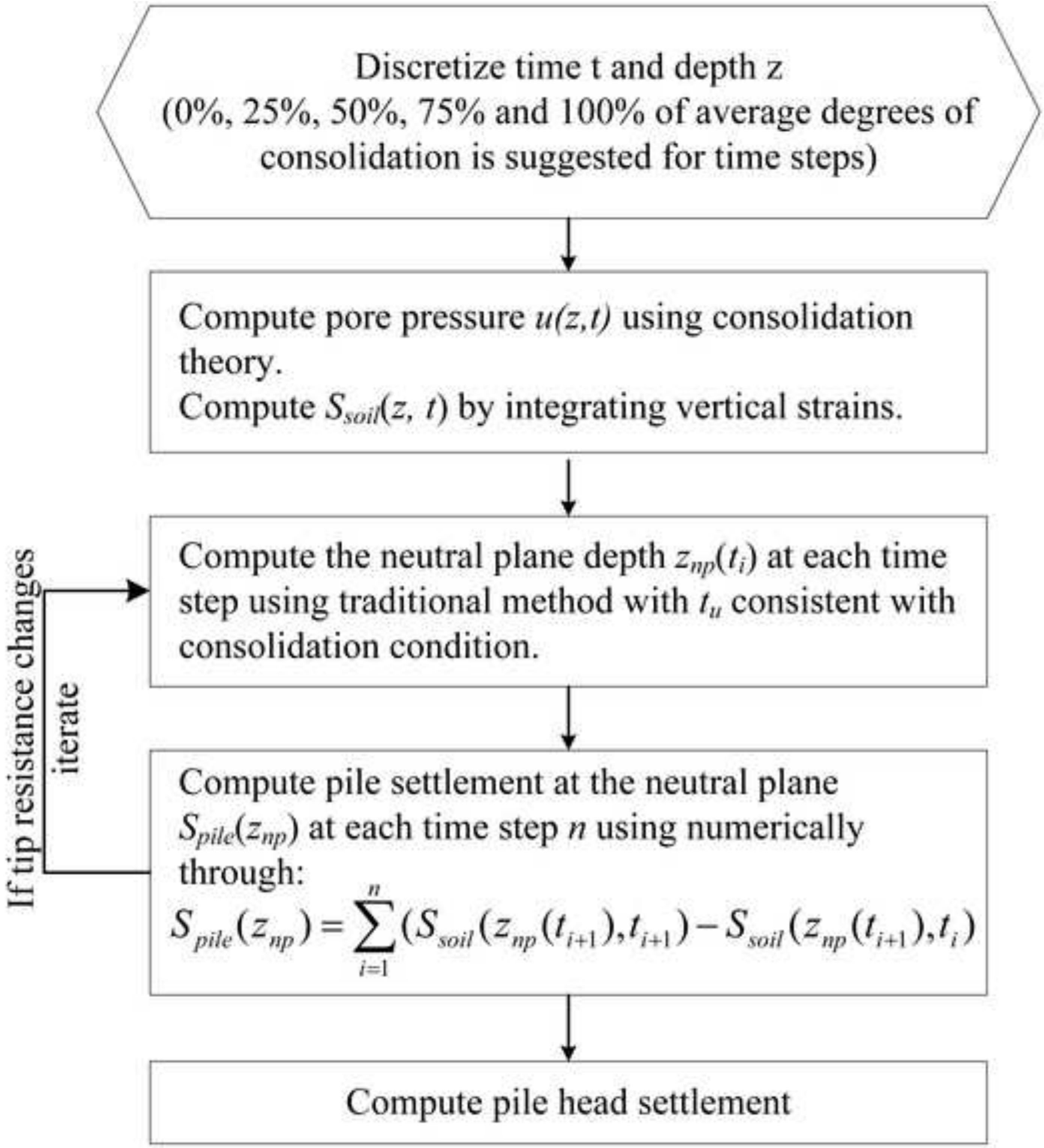

Figure 12
Click here to download high resolution image

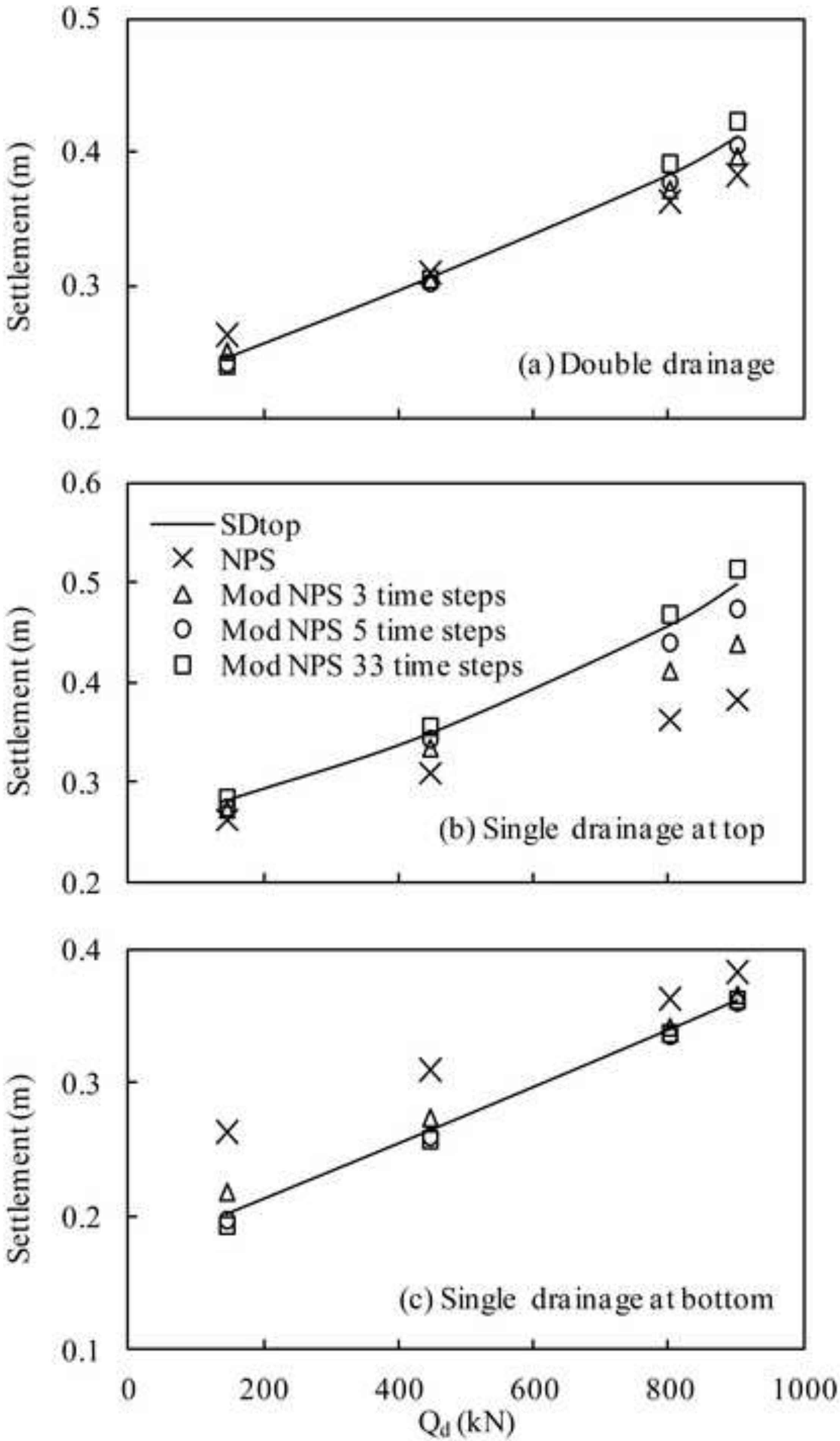

Figure 13
Click here to download high resolution image

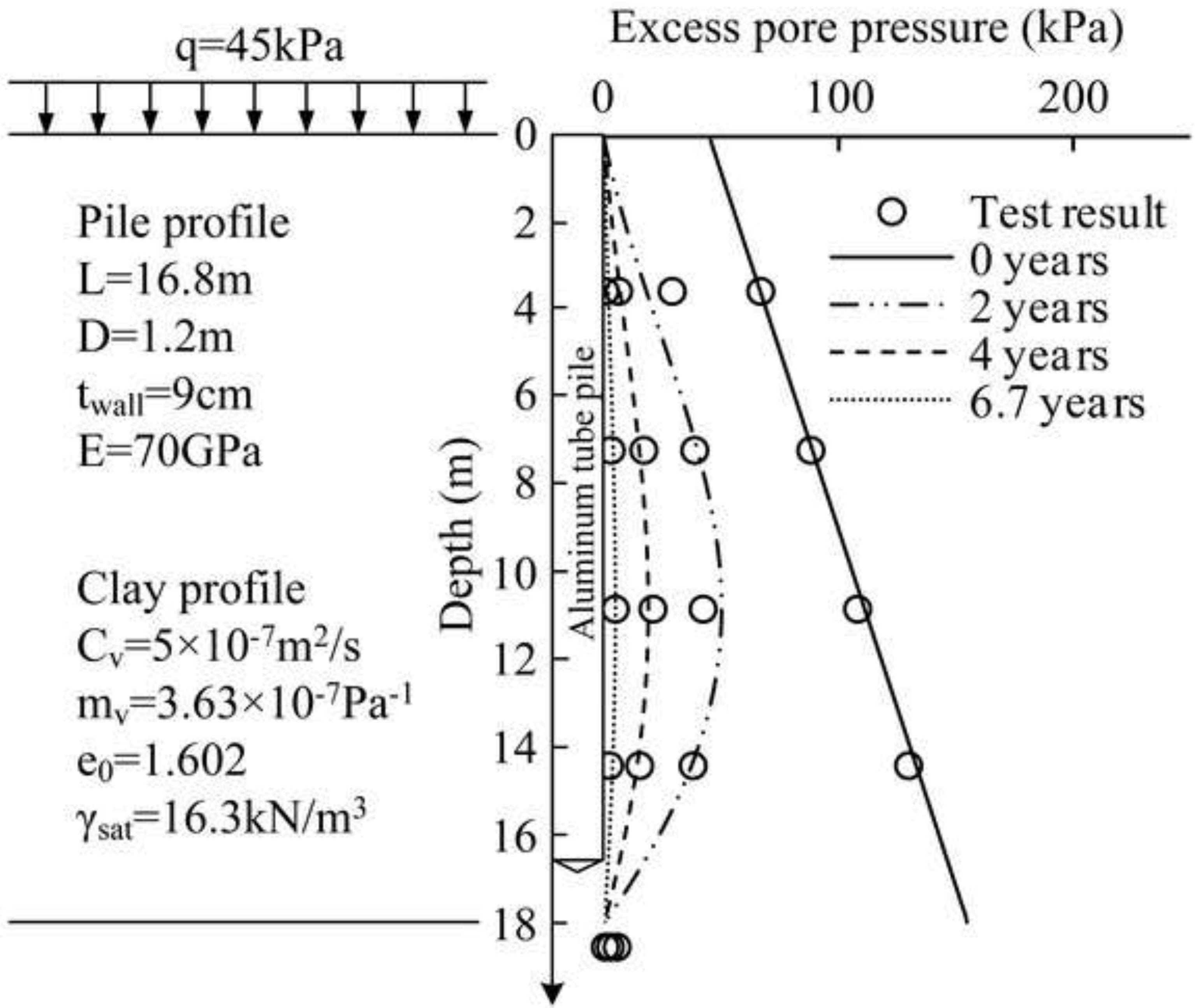

Figure 14
Click here to download high resolution image

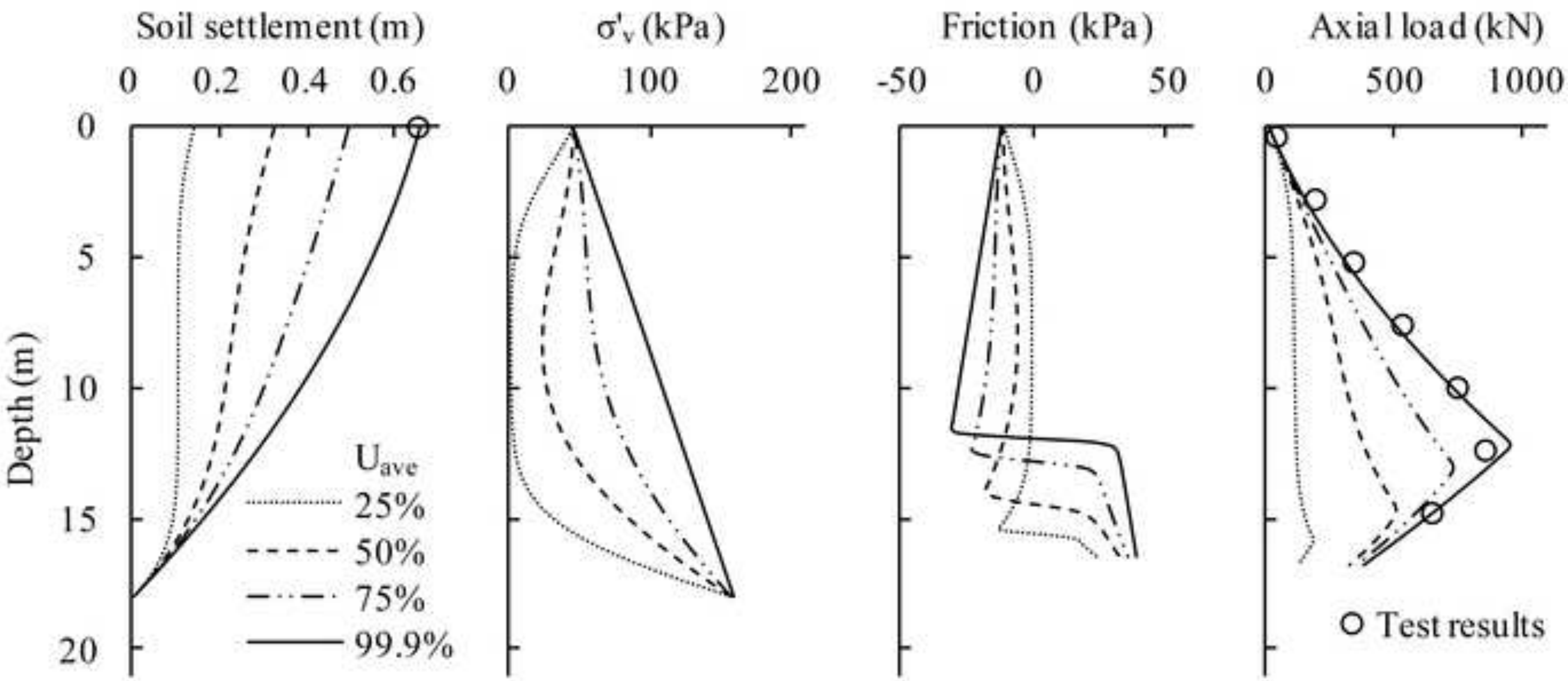

Figure 15
Click here to download high resolution image

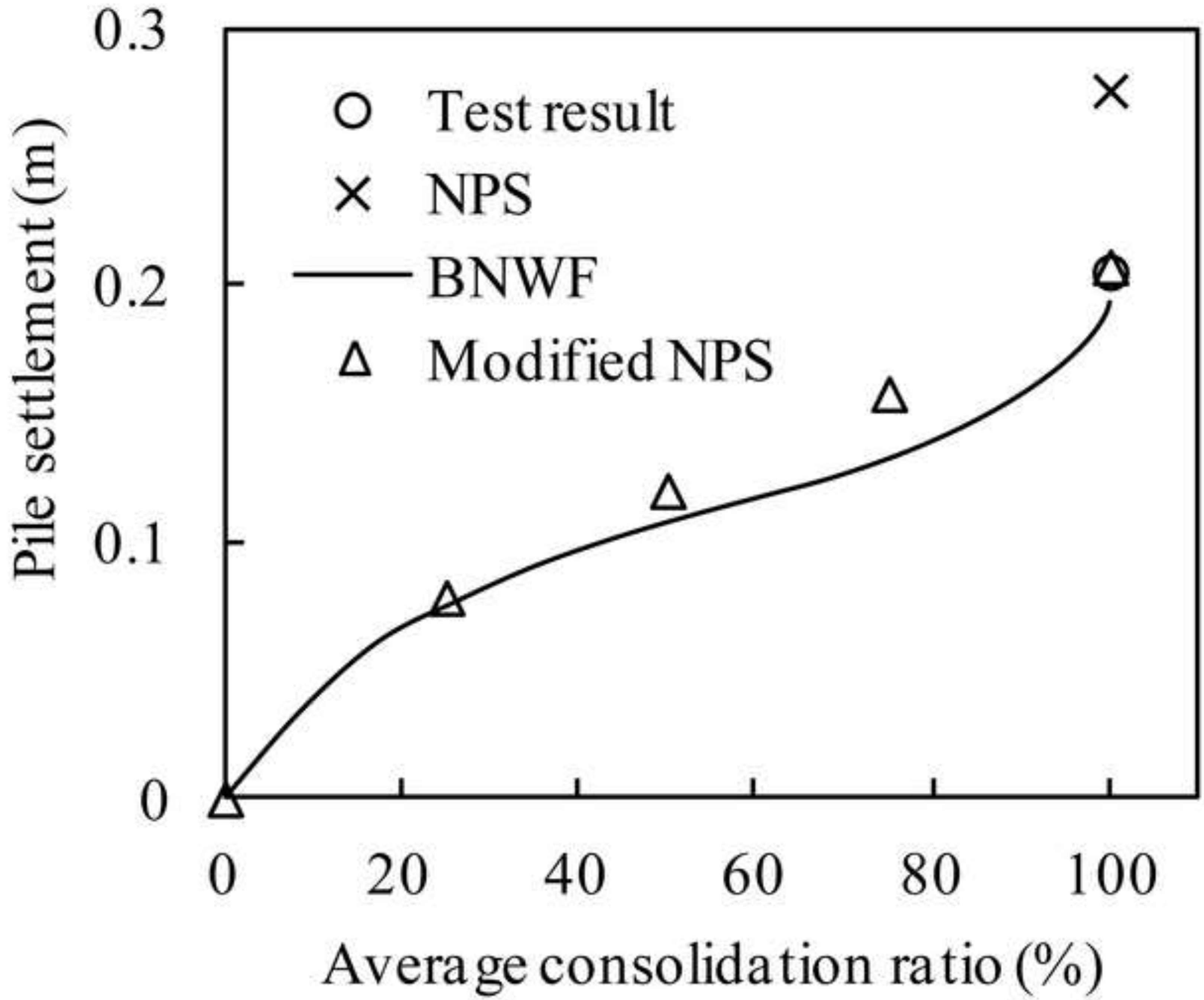

List of figures

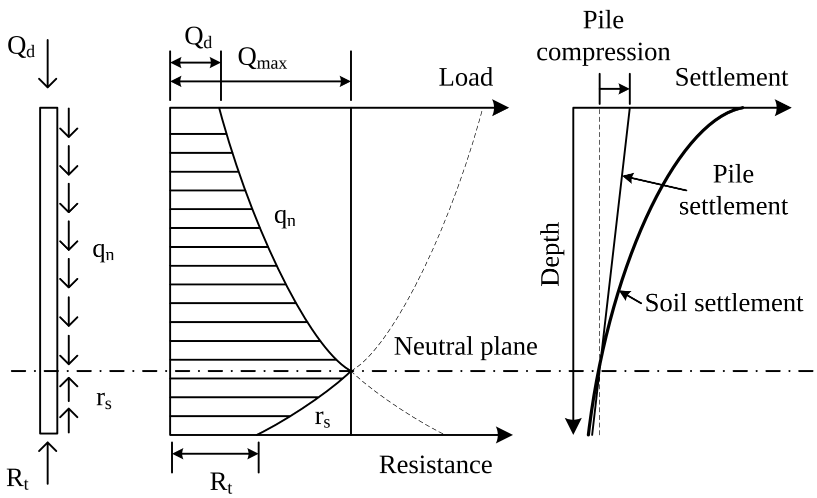

Fig. 1. Illustration of the neutral plane solution (after Fellenius 1984)

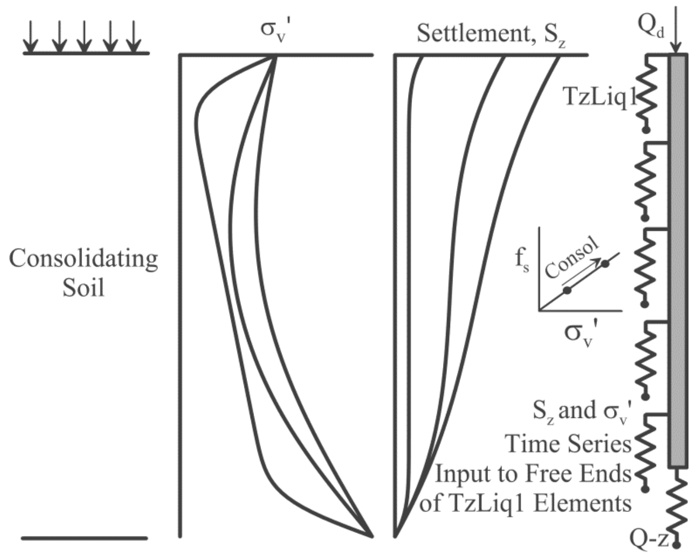

Fig. 2. Schematic of BNWF method using TzLiq1 material.

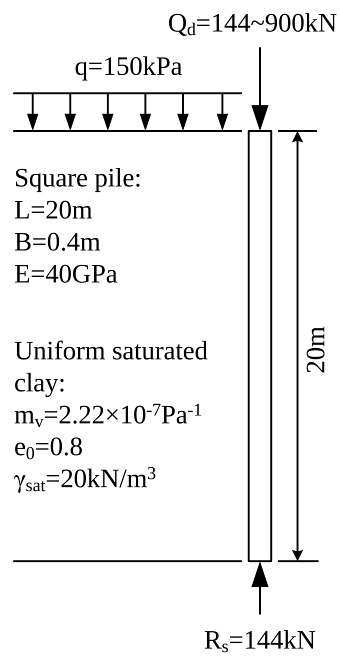

Fig. 3. Basic pile and soil setup for the example analyses

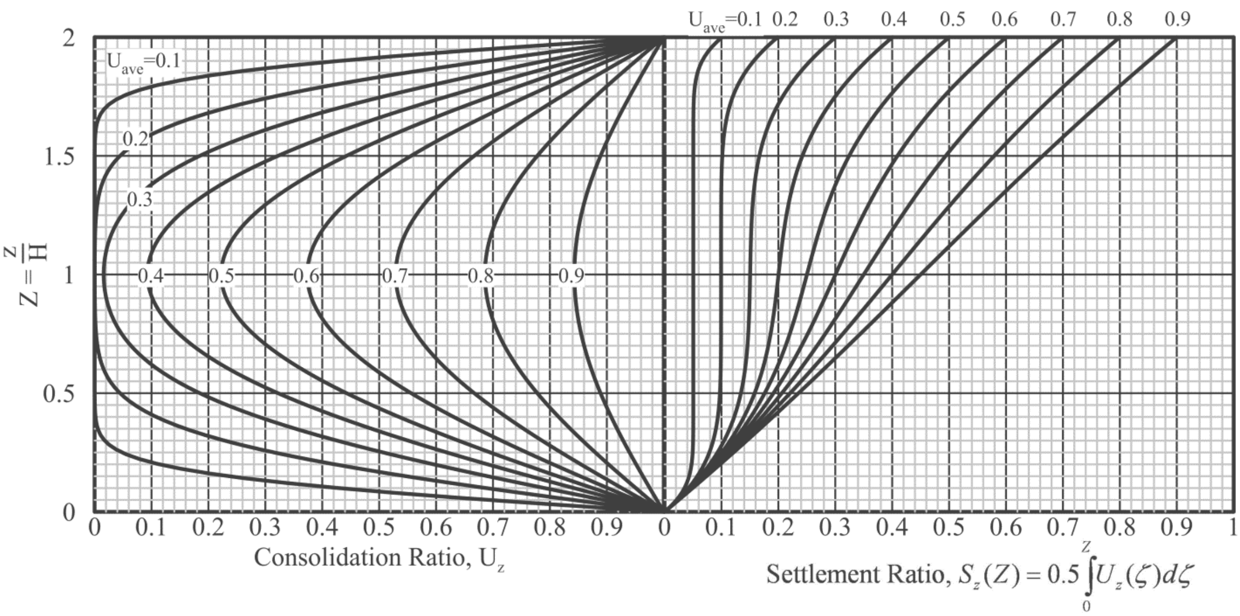

Fig. 4. Pore pressure and settlement isochrones from Terzaghi's one dimensional consolidation theory.

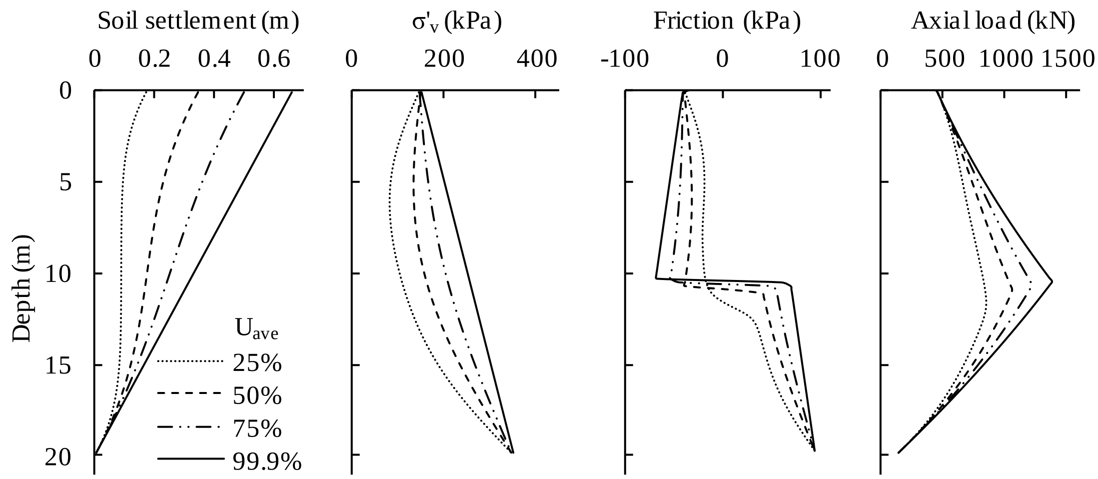

Fig. 5. Soil and pile responses at different average degrees of consolidation in a double drainage soil profile. Q_d=445kN.

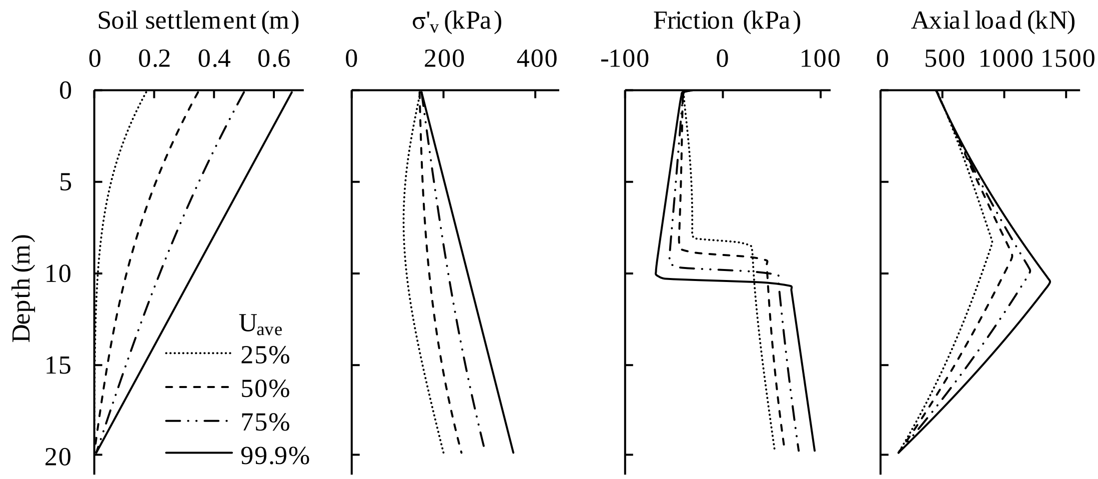

Fig. 6. Soil and pile responses at different average degrees of consolidation in a single drainage through the top soil profile. Q_d=445kN.

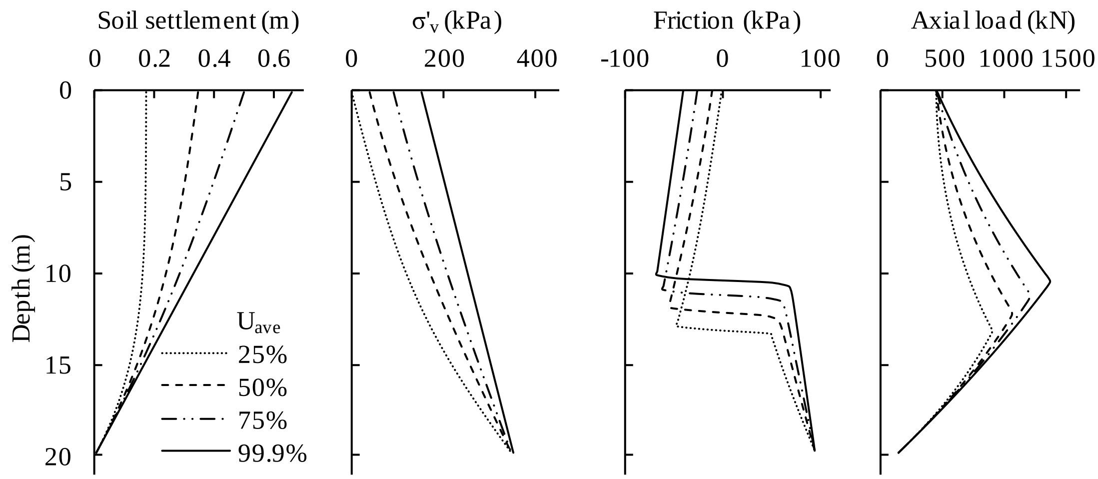

Fig. 7. Soil and pile responses at different average degrees of consolidation in a single drainage through the bottom soil profile. Q_d=445kN.

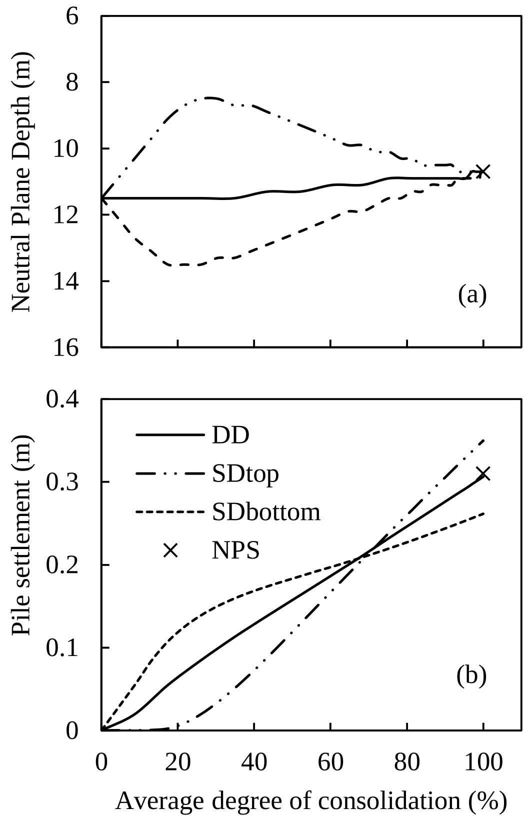

Fig. 8. Neutral plane depth and pile settlement histories. Q_d=445kN. (a) Neutral plane depth versus average degree of consolidation. (b) Pile settlement versus average degree of consolidation compared with conventional neutral plane solution

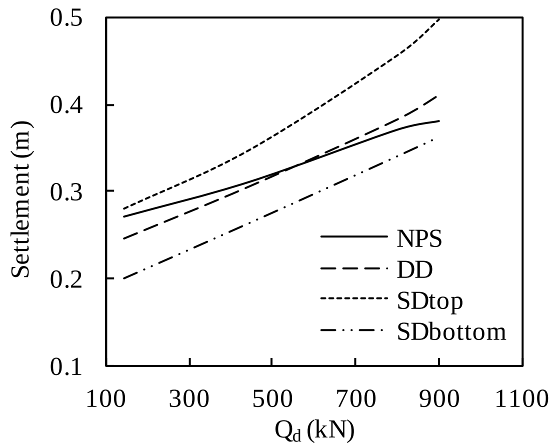

Fig. 9. Pile settlements versus pile head load in the neutral plane solution compared with BNWF results under different drainage conditions

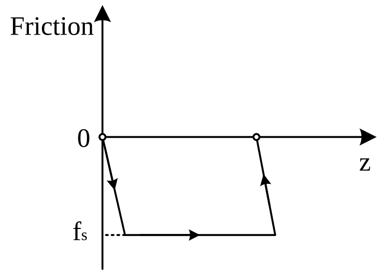

Fig. 10. Force-displacement behavior between soil and pile considering elasto-plasticity

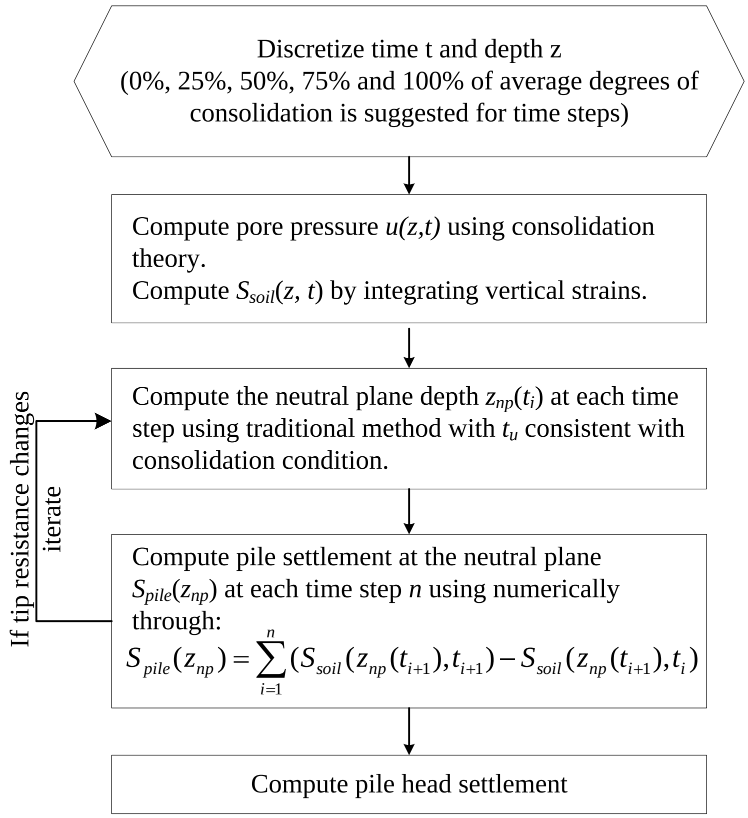

Fig. 11. Flow chart of the proposed modified neutral plane method

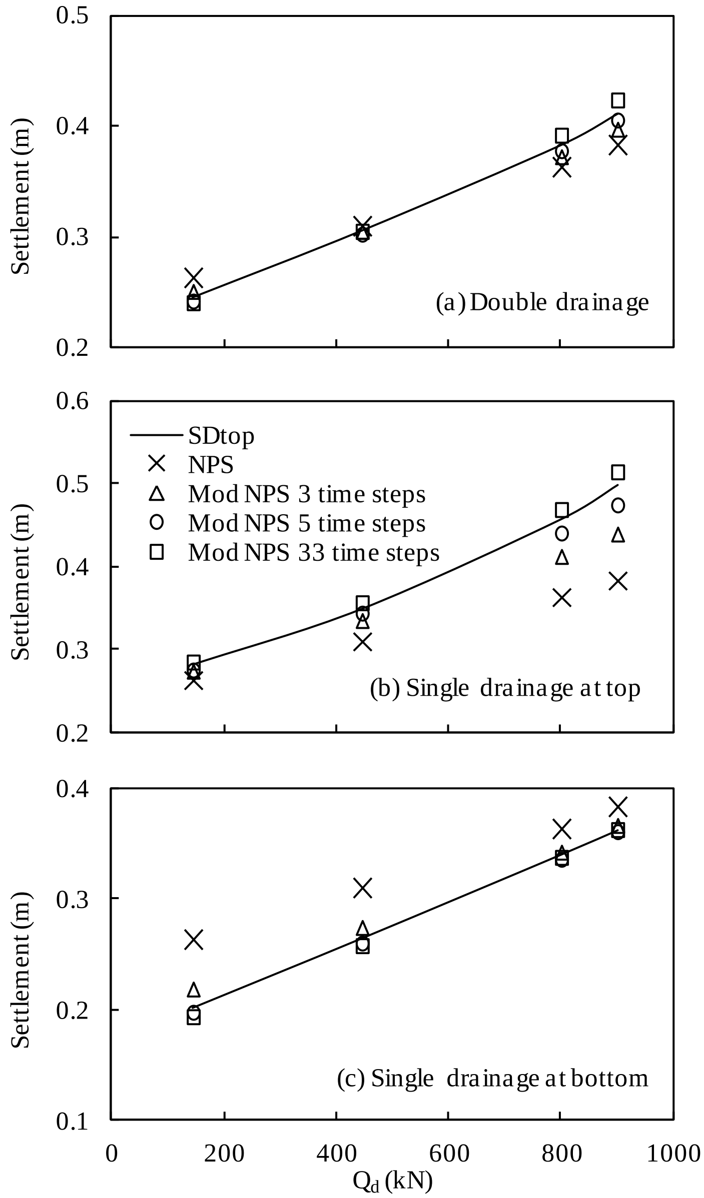

Fig. 12. Comparison between settlements calculated by the BNWF method and the modified neutral plane method using different number of intervals (including the conventional neutral plane solution).

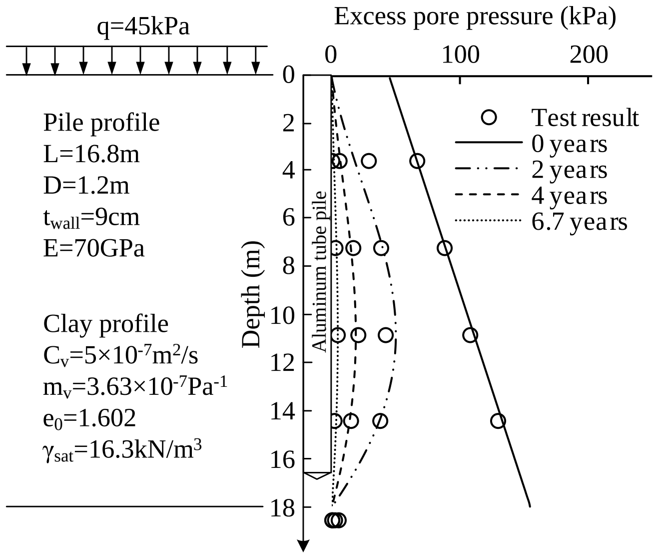

Fig. 13. Excess pore pressure isochrones from Terzaghi's one dimensional consolidation theory compared with test data (test data from Lam et al., 2009)

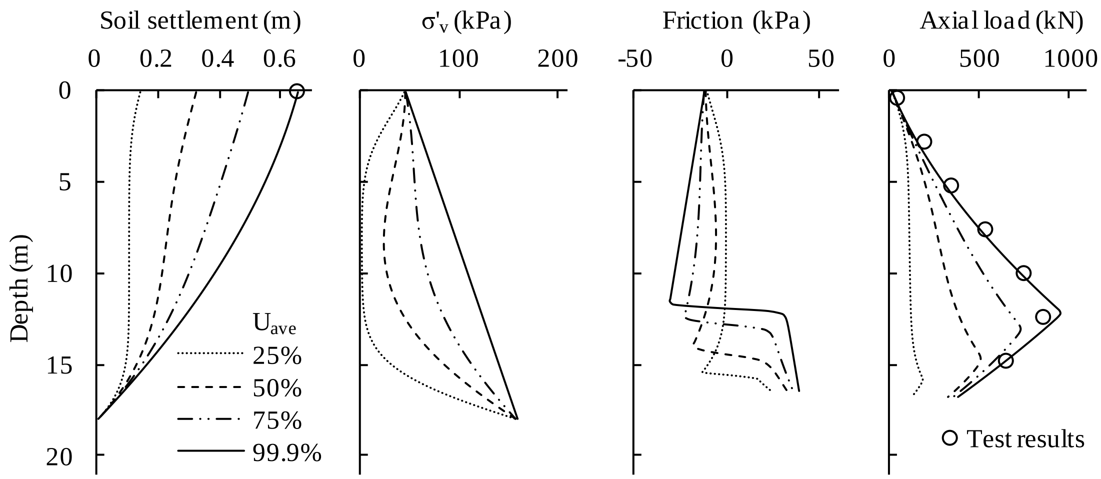

Fig. 14. Soil and pile responses at different average degrees of consolidation compared with centrifuge test data (test data from Lam et al., 2009)

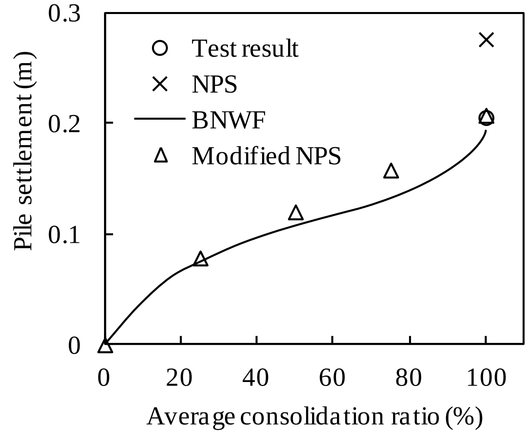

Fig. 15. Pile settlement results from test data and different calculation methods (test data from Lam et al., 2009)